JOURNAL OF GEOPHYSICAL RESEARCH, VOL. 86, NO. B4, PAGES 2737-2755, APRIL 10, 1981

An Oxygen Isotope Profile in a Section of Cretaceous Oceanic Crust, Samail Ophiolite, Oman: Evidence for $\delta^{18}O$ Buffering of the Oceans by Deep (>5 km) Seawater-Hydrothermal Circulation at Mid-Ocean Ridges

ROBERT T. GREGORY AND HUGH P. TAYLOR, JR.

Division of Geological and Planetary Sciences, California Institute of Technology, Pasadena, California 91125

Isotopic analyses of 75 samples from the Samail ophiolite indicate that pervasive subsolidus hydrothermal exchange with seawater occurred throughout the upper 75% of this 8-km-thick oceanic crustal section; locally, the H_2O even penetrated down into the tectonized peridotite. Pillow lavas ($\delta^{18}O$ = 10.7 to 12.7) and sheeted dikes (4.9 to 11.3) are typically enriched in ^{18}O, and the gabbros (3.7 to 5.9) are depleted in ^{18}O. In the latter rocks, water/rock $\leq$ 0.3, and $\delta^{18}O_{cpx} \approx 2.9 + 0.44\ \delta^{18}O_{feld}$, indicating pronounced isotopic disequilibrium. The mineral $\delta^{18}O$ values approximately follow an exchange (mixing) trajectory which requires that plagioclase must exchange with H_2O about 3 to 5 times faster than clinopyroxene. The minimum $\delta^{18}O_{feld}$ value (3.6) occurs about 2.5 km below the diabase-gabbro contact. Although the gabbro plagioclase appears to be generally petrographically unaltered, its oxygen has been thoroughly exchanged; the absence of hydrous alteration minerals, except for minor talc and/or amphibole, suggests that this exchange occurred at $T > 400°$–$500°C$. Plagioclase $\delta^{18}O$ values increase up section from their minimum values, becoming coincident with primary magmatic values near the gabbro-sheeted diabase contact and reaching 11.8 in the diabase dikes. These ^{18}O enrichments in greenschist facies diabases are in part due to exchange with strongly ^{18}O-shifted fluids, in addition to retrograde exchange at much lower temperatures. The $\delta^{18}O$ data and the geometry of the mid-ocean ridge (MOR) magma chamber require that two decoupled hydrothermal systems must be present during much of the early spreading history of the oceanic crust (approximately the first 10^6 years); one system is centered over the ridge axis and probably involves several convective cells that circulate downward to the roof of the magma chamber, while the other system operates underneath the wings of the chamber, in the layered gabbros. Upward discharge of ^{18}O-shifted water into the altered dikes from the lower system, just beyond the distal edge of the magma chamber, combined with the effects of continued low-T hydrothermal activity, produces the ^{18}O enrichments in the dike complex. Integrating $\delta^{18}O$ as a function of depth for the entire ophiolite establishes (within geologic and analytical error) that the average $\delta^{18}O$ (5.7 $\pm$ 0.2) of the oceanic crust did not change as a result of all these hydrothermal interactions with seawater. Therefore the net change in $\delta^{18}O$ of seawater was also zero, indicating that seawater is buffered by MOR hydrothermal circulation. Under steady state conditions the overall bulk ^{18}O fractionation (Δ) between the oceans and primary mid-ocean ridge basalt magmas is calculated to be +6.1 $\pm$ 0.3, implying that seawater has had a constant $\delta^{18}O \approx -0.4$ (in the absence of transient effects such as continental glaciation). Utilizing these new data on the depth of interaction of seawater with the oceanic crust, numerical modeling of the hydrothermal exchange shows that as long as worldwide spreading rates are greater than 1 km^2/yr, ^{18}O buffering of seawater will occur. These conclusions can be extended as far back in time as the Archean (> 2.6 eons) with the proviso that Δ may have been slightly smaller (about 5?) because of the overall higher temperatures that could have prevailed then. Thus ocean water has probably had a constant $\delta^{18}O$ value of about -1.0 to $+1.0$ during almost all of earth's history.

INTRODUCTION

The purpose of this study is to determine the oxygen isotope relationships in minerals and rocks throughout a complete section of oceanic crust. Such a characterization is important because of the profound effects that hydrothermal circulation at mid-ocean ridges (MOR) must have upon (1) the isotopic and chemical composition of ocean water through geologic time and (2) the isotopic and chemical composition of the oceanic crust that is recycled into the mantle at subduction zones. Oxygen isotope studies of ancient oceanic lithosphere preserved in ophiolite complexes [*Coleman*, 1977] can provide a framework for studying the time-averaged effects of seawater circulation in 'fossil' hydrothermal systems associated with marine spreading centers. Such studies also make it easier to interpret geochemical information gained from dredge samples and from seafloor hot spring studies [*Muehlenbachs and Clayton*, 1972*a*; *Corliss et al.*, 1979].

Abundant evidence of hydrothermal alteration has now been observed in samples dredged from the seafloor and collected from ophiolite complexes [*Coleman*, 1977; *Wenner and Taylor*, 1978; *Melson and Van Andel*, 1966, *Heaton and Sheppard*, 1977; *Muehlenbachs and Clayton*, 1972*b*]. Heat flow anomalies at mid-ocean ridges also require the existence of such hydrothermal systems, and direct evidence of discharge of thermal waters has now been observed with the Alvin submersible [*Corliss et al.*, 1979; *Edmond et al.*, 1979].

Previous $^{18}O/^{16}O$ studies of suboceanic and ophiolitic terranes indicate the existence of samples that exhibit both ^{18}O enrichments (e.g., pillow lavas) and ^{18}O depletions (e.g., gabbros) relative to the primary magmatic $\delta^{18}O$ values [*Heaton and Sheppard*, 1977; *Magaritz and Taylor*, 1976*a*; *Spooner et al.*, 1974; *Muehlenbachs and Clayton*, 1971]. These $\delta^{18}O$ changes have in general all been attributed to subsolidus hydrothermal alteration, at relatively low temperatures or high temperatures, respectively.

Muehlenbachs and Clayton [1976] have proposed that the

Paper number 80B0711.
0148-0227/81/080B-0711$01.00

^{18}O fluxes into seawater from continental weathering and from dehydration water cycled through subduction zones and outgassed in magmatic arcs are (1) opposite in sign, (2) roughly equal in magnitude, and (3) a factor of 10 smaller than the potential ^{18}O flux due to marine-hydrothermal interactions at ridges. If these concepts are valid, it is clear that the latter will ultimately determine the $\delta^{18}O$ value of the oceans. *Muehlenbachs and Clayton* [1976] pointed out that if the ^{18}O fluxes resulting from high-temperature alteration processes (which produce an ^{18}O enrichment of seawater) exactly cancel out the ^{18}O fluxes due to low-temperature interaction (which result in an ^{18}O depletion of seawater), then the average steady state isotopic fractionation between seawater and oceanic crust would hold seawater at its present-day $\delta^{18}O$ value. Ocean water would be 'buffered' at this value as long as extensive hydrothermal circulation at the mid-ocean ridges continued. *Perry et al.* [1978], however, have proposed that the $\delta^{18}O$ of seawater has changed with time and was controlled by weathering and low-temperature hydrothermal alteration on the seafloor, during most of the earth's history.

Ophiolite complexes are now generally recognized to represent fragments of ancient oceanic crust and mantle [*Coleman,* 1977]; $^{18}O/^{16}O$ studies of such complexes thus can provide a test of the *Muehlenbachs and Clayton* [1976] hypothesis. However, stable isotope studies of ophiolites have up to now been mainly concerned with the uppermost sections of diabase dikes and pillow lavas and with the serpentinized peridotites [*Wenner and Taylor,* 1978; *Heaton and Sheppard,* 1977; *Spooner et al.,* 1974; *Magaritz and Taylor,* 1974]. They have generally not addressed the problem of the depth of penetration of marine-hydrothermal ^{18}O effects into the cumulate gabbro sections that are presumably equivalent to oceanic layer 3. In order to define the overall average $\delta^{18}O$ value of the oceanic crust it is crucial to determine the volume of ^{18}O-depleted cumulates produced during deep hydrothermal circulation within a typical slice of oceanic crust.

Low-^{18}O basalts and gabbros produced by interaction with low-^{18}O meteoric groundwaters have been reported at many continental localities [*Taylor,* 1968; *Taylor and Forester,* 1971; *Taylor,* 1971; *Forester and Taylor,* 1977]. These low-^{18}O intrusive rocks commonly occur as epizonal intrusions emplaced into highly fractured and permeable volcanic country rocks. The intrusions act as gigantic heat engines which drive hydrothermal circulation of meteoric water through the rocks. Ophiolite gabbro complexes are geologically analogous to some of these ^{18}O-depleted, continental igneous complexes. Examples are subvolcanic, epizonal layered gabbro bodies intruded into contemporaneous volcanic piles associated with sheeted dike swarms: the Jabal at Tirf complex in the Red Sea rift zone [*Taylor and Coleman,* 1977]; the Skaergaard intrusion–East Greenland dike swarm [*Taylor and Forester,* 1979] and the Scottish Hebrides intrusive ring plutons, both emplaced into plateau basalt lavas and both associated with the initial opening of the North Atlantic Ocean [*Taylor and Forester,* 1971; *Forester and Taylor,* 1977]; and the present-day, postglacial basaltic and rhyolitic volcanism in the Eastern Rift Zone of Iceland [*Muehlenbachs et al.,* 1974]. These all represent classic areas of low-^{18}O igneous rocks produced by interaction with circulating hydrothermal fluids [*Taylor,* 1980].

The major differences (ignoring scale) between these continental environments and the marine ophiolite complexes are the following: (1) In the latter, ocean water with a $\delta^{18}O \approx 0$ instead of meteoric water with a $\delta^{18}O \approx -5$ to -15 is the source of the hydrothermal fluid. (2) On the seafloor the spreading rates and rate of production of new crust are typically much more rapid. The difference between hydrothermal fluids derived from seawater or from meteoric water is important, because the contrast in $\delta^{18}O$ between seawater and primary basaltic magma is only about 6‰, much less than the contrast between meteoric waters and igneous rocks. The isotopic effects of marine-hydrothermal alteration are therefore much more difficult to detect and interpret, because the 'signal-to-noise' ratio is so much smaller. The much more dynamic MOR spreading processes also produce an oceanic crustal ^{18}O profile that represents superposition of various time, space, and temperature regimes. As it moves away from the spreading center into a cooler environment, the oceanic crust experiences an aging process which has no direct counterpart in the continental systems that have been investigated to date. The more active spreading regimes also probably lead to more intense fracturing and collapse features, resulting in higher permeabilities and thus leading to deeper and more vigorous convective circulation of the hydrothermal fluids.

GEOLOGICAL RELATIONSHIPS AND SAMPLING

General Features

The Samail ophiolite, Sultanate of Oman, was selected for this study because it is probably the largest and best exposed ophiolite complex in the world. It crops out in an area of major topographic relief throughout a desert region comparable in size to the Sierra Nevada batholith (Figure 1). Not only is the Samail ophiolite large and well exposed, but in places the thrust slices of oceanic crust are essentially internally undeformed [*Coleman,* 1977]. Individual members of the ophiolite stratigraphic succession have thicknesses comparable to their typical oceanic counterparts.

The Samail ophiolite formed in the Hawasina ocean basin, which probably existed as an entity from latest Permian to latest Cretaceous time [*Glennie et al.,* 1974]. The Hawasina Ocean was a portion of the great Tethys seaway, and the Samail ophiolite apparently formed at a Tethyan mid-ocean ridge during Cretaceous spreading [*Reinhardt,* 1969; *McCulloch et al.,* 1980; *Tilton et al.,* 1981]. The ophiolite is the highest tectonic member of a series of nappes which were transported southward during Late Cretaceous time across the Arabian continental margin [*Glennie et al.,* 1974]. A Maestrichtian-Tertiary shallow water marine limestone unconformably overlies the ophiolite and provides evidence for a minimum emplacement age [*Glennie et al.,* 1974]. Zircon ages of 95 ± 2 m.y. [*Tilton et al.,* 1981], together with a 90-m.y. K-Ar age from an amphibolite aureole beneath the Samail thrust, bracket the initial detachment age within the interval 95–90 m.y. [*Lanphere et al.,* 1981]. Maestrichtian shales from the underlying melange require that last movement of the Samail nappe is probably no older than 65–71 m.y. [*Hopson et al.,* 1981].

The present-day relief of the Oman Mountains is due to a Pliocene folding event contemporaneous with folding in the Zagros belt of Iran. Note that the Samail ophiolite was not emplaced into its present position by subduction followed by buoyant uplift along reverse faults at the front of an andesitic arc [*Coleman,* 1981]. Basal contact relations prove the existence of an episode of early movement while the lower portion of the Samail nappe was hot enough to produce extensive contact metamorphism, followed by a later movement under much lower temperature conditions. Emplacement was thus a

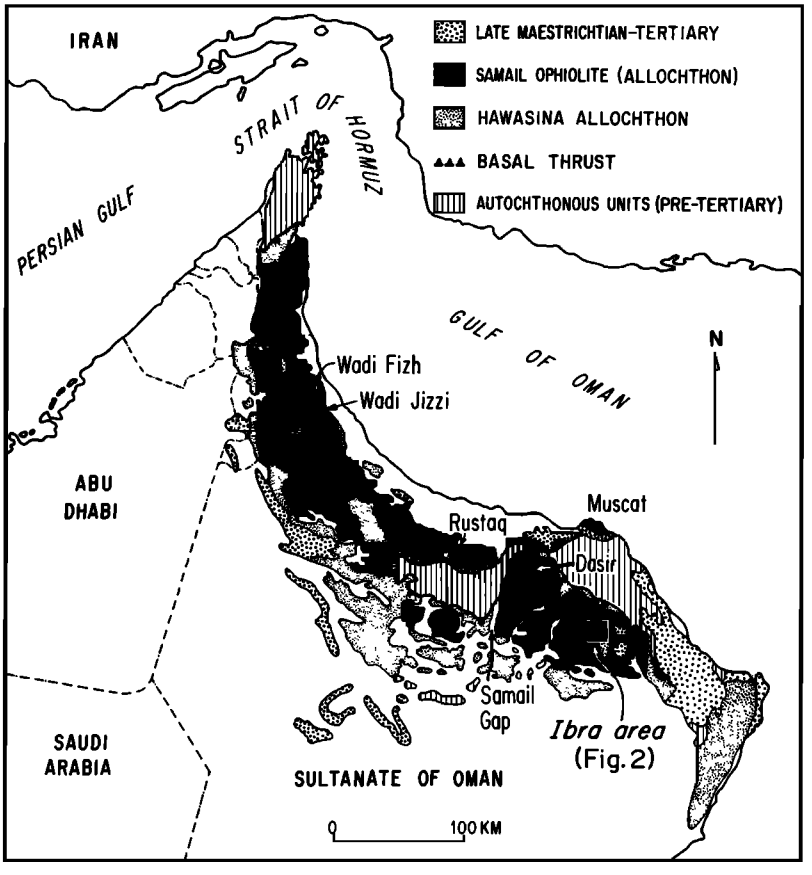

Fig. 1. Generalized geologic map of the Samail ophiolite, Oman, showing an inset of the Ibra area (modified after *Glennie et al.* [1974]).

two-stage process that apparently culminated in gravity sliding of the ophiolite mass onto the Arabian continental margin [*Coleman*, 1981; *Boudier and Coleman*, 1981].

Except for the basal amphibolite, none of the metamorphic assemblages observed in the oceanic crustal section are due to metamorphism associated with obduction. There is no evidence of any postemplacement Tertiary igneous activity in the Oman Mountains or along the eastern Arabian continental margin. Rare diabase and gabbro dikes with chilled margins crosscut the Samail peridotite and the high-temperature contact aureole but do not crosscut the allochthonous Hawasina melange or the autochthonous Hajar group, suggesting a seafloor, pre-Maestrichtian origin. Therefore excluding the very low-temperature, late stage serpentinization of the peridotite, which was apparently caused by meteoric waters [*Barnes et al.*, 1978], all of the hydrothermal metamorphism of the Oman ophiolite oceanic crustal section is attributed to seafloor processes.

Geology and Petrology of the Ibra Section

The samples analyzed in this study come from the Ibra area, southeastern Oman Mountains (Figure 2). The geology of this area is discussed in detail by *Hopson et al.* [1981], so only those geological relationships necessary for this discussion will be reviewed here.

Samples were collected from two Wadis (Saq and Kadir) which drain the north limb of a syncline (Figure 2). The peridotite-gabbro contact (the fossil 'Moho') crops out at the heads of the drainages near the crest of the range. Both wadis empty onto a pediment dotted with low hills of sheeted diabase dikes. The pillow lavas form relatively poor outcrops to the south, near the axis of the syncline.

The Wadi Saq gabbro section is truncated at its base by a late, low-angle fault which results in an atypically thin (3.5 km) gabbro section here [*Hopson et al.*, 1981]. However, this section was picked for study because of the abundant sheeted diabase dikes which form well-exposed outcrops along this traverse. The Wadi Kadir traverse has a complete gabbro section (≈5 km thick) but has limited exposures of sheeted diabase dikes. The combination of the two sections gives a virtually complete cross section through the oceanic crust.

Samples of gabbro dikes which crosscut the peridotite but are not chilled against it were collected from a traverse through the peridotite roughly collinear with the east fork of Wadi Kadir, just north of the area shown in Figure 2, in collaboration with R. G. Coleman and F. Boudier. The latter workers are making a detailed structural and petrologic study along this section through the peridotite [*Boudier and Coleman*, 1981].

From bottom to top, a generalized stratigraphic section through the ophiolite in the Ibra area consists of tectonized harzburgite peridotite; a thin basal zone of olivine-clinopyroxene cumulates (wehrlites); followed by 3–5 km of olivine-clinopyroxene-plagioclase cumulates (layered gabbros); grading into less than 1 km of plagioclase-hornblende ± clinopyroxene ± olivine + magnetite, noncumulate, high-level gabbro. Over an abrupt transition interval (<10 m thick) a zone of high-level gabbro with 10% diabase dikes gives way to a

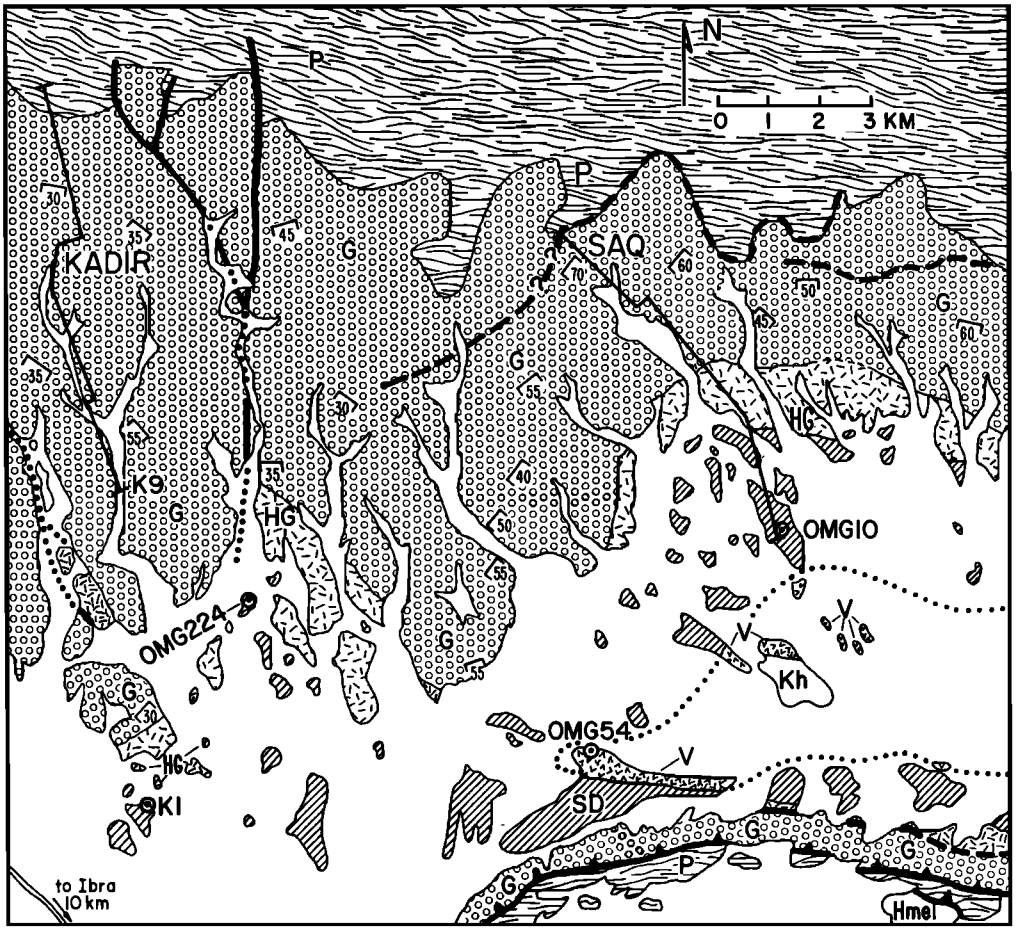

Fig. 2. Geologic map of the Ibra area [after *Hopson et al.*, 1981], showing the location of the Wadi Saq and Wadi Kadir sections and other samples analyzed in this study and in the study of *McCulloch et al.* [1981]. P (wavy pattern), peridotite (tectonized harzburgite and dunite); G, layered cumulate gabbro; HG, high-level, noncumulate gabbro; SD, sheeted diabase dike complex—in the Wadi Saq area the lined pattern is approximately parallel to the strike of the sheeted dikes; V, pillow basalts; Kh, Hawasina pelagic sediments; and Hmel, Hawasina melange. Heavy black lines are faults; dotted contact indicates concealed SD-V contact, which defines the position of the Ibra syncline.

100% sheeted diabase dike complex that is 1 to 2 km thick. Above the diabase dike complex is a relatively thin section of pillow lavas (<700 m thick), and above the pillow lavas, and in some cases intercalated with the pillow lavas are rare exposures of red chert.

Alteration minerals are abundant in the pillow basalt section (now altered to zeolite facies), in the diabase section (lower greenschist to lower amphibolite facies), and in the high-level gabbro (amphibolite facies). Igneous textures are generally extremely well preserved, indicative of essentially static, hydrothermal metamorphism. The lower cumulates commonly exhibit alteration minerals that are visible only under the microscope, such as very minor talc-magnetite alteration of olivine. The cumulate rocks generally appear to be petrographically unaltered (but they are, in fact, highly altered; see below). The alteration mineral assemblages present in the diabases and pillow lavas are similar to those described in most other ophiolite complexes throughout the world [*Coleman*, 1977].

Experimental Results

Oxygen was liberated from silicates using the fluorine technique described by *Taylor and Epstein* [1962]. The results are reported in δ notation in parts per mil (‰), where

$$\delta^{18}O_{sample} = \left(\frac{^{18}O/^{16}O_{sample}}{^{18}O/^{16}O_{standard}} - 1 \right) 1000$$

Precision is better than 0.2‰, and raw $\delta^{18}O$ values are corrected to the SMOW scale using Caltech rose quartz $\delta^{18}O$ = 8.45. NBS-28 has $\delta^{18}O$ = +9.60 on this scale. Hydrogen was liberated from silicates by the technique described by *Godfrey* [1962], and results are also reported relative to SMOW in permil.

The $\delta^{18}O$ and δD data are presented in Table 1. Plagioclase samples were analyzed in larger numbers than other minerals because feldspar is more sensitive to subsolidus hydrothermal ^{18}O exchange than any other silicate [*Taylor*, 1968; *Taylor and Forester*, 1971]. Therefore plagioclase was separated from all medium-to-coarse grained intrusive samples either magnetically or by hand picking. Pyroxene and amphibole mineral separates were obtained from magnetic concentrates that were further purified by hand picking. Quartz from plagiogranites was separated by hand picking and HF treatment.

The $\delta^{18}O$ values of whole-rock samples were either analyzed directly from representative splits made from interior

TABLE 1. Oxygen Isotope Analyses, Mineralogy, and Calculated Values of $\delta^{18}O_{H_2O}$ and Water/Rock Ratio for Minerals and Rocks of the Samail Ophiolite Complex, Oman

Sample*	Mineralogy†	$\delta^{18}O_f$	$\delta^{18}O_{px}$	$\delta^{18}O_{other}$	$\delta^{18}O_{rock}$	$\delta^{18}O$ of H_2O Equation‡	w/r ‖
			Pillow Basalt (100°-200°C)				
OMG 54 (I)	*f, pg, op, z,* [ca, *sa*]				12.7	−0.6–5.8	4.2
OMG 12-1 (J)	*f, op, e, z,* px				12.5	−0.8–5.6	3.2
L 2.2 125 (J)	*f, q, op, c*[*sp*]				10.7	−2.6–3.8	1.2
L.2.2 144 (J)	*f, q, op, c,* [*e, sp*]				10.7	−2.6–3.8	1.2
			Sheeted Diabase (250°-400°C)				
OMG 6 (S)	*f, c, q, e, op,* [*ca, l*]				9.3	4.3–7.6	n.d.
OMG 10 (S)	*f, a, c, q, e, op,* [*sp, ca*]	11.8			8.5	3.5–6.8	n.d.
OMG 8 (S)	*f, op, c, e, q*				8.2	3.2–6.5	n.d.
OMG 7a (S)	*f, op, c, e, q*				7.9	2.9–6.2	n.d.
OMG 7b (S)	*f, op, c, e, q*				8.3	3.3–6.6	n.d.
OMG 5-3 (S)§	*f, a, c, op, q,* [*ca, e*]	5.6			4.9	−0.1–3.2	1.2
OMG 5-1 (S)	*f, a, e, c, q, op*				11.3	6.3–9.6	n.d.
K 1 (K)	*f, a, op, c, q, e*				6.8	1.8–5.1	n.d.
			High-Level Gabbro (400°-600°C				
OMG 71-1 (S)§	f, h, *a,* [px, op, *e*]	6.8		5.0 (a + h)	5.9**	4.9–7.1	n.d.
OMG 70 (S)	f, px, ol [h, op, *a, c, t*]	6.5				4.9–7.0	n.d.
OMG 64 (S)	f, px, h, ol. [op, *a, c, t*]	4.3				2.4–4.6	0.5
OMG 224-2 (K)	f, h, op, *a, c,* [*p*]	4.5		2.6 (a + h)	3.7	2.2–4.5	0.4
			Cumulate Gabbro (400°-600°C)				
OMG 66 (S)	f, px, ol, [h, *op, a, t, s*]	5.8				4.2–6.3	0.04
OMG 65 (S)	f, px, ol, [*op, t, h*]	4.2				2.5–4.9	0.6
OMG 63 (S)	f, px, ol, [*op, t, h*]	4.1	4.3		4.2**	2.7–4.7	0.6
OMG 62 (S)	f, px, ol, [*op, t*]	4.4			4.5	2.8–4.9	0.5
OMG 68 (S)	f, px, ol, [*h, t, c, op, s*]	3.6	4.1		3.7**	2.0–4.2	0.9
OMG 58 (S)	f, px, ol, [*c, s*]	5.3	4.9		5.1**	3.7–5.8	0.2
OMG 67 (S)	f, px, ol, [*t, op, s, c*]	6.0	5.7		6.0**	4.4–6.5	n.d.
OMG 58a (S)	f, px, ol, [*op, s*]	4.7			4.5	3.1–5.1	0.4
OMG 58b(S)	f, px, ol, [*op, s*]	6.0				4.3–6.4	n.d.
OMG 57 (S)	f, px, ol, [*s, p, hg*]	6.6	5.7		6.4	5.1–7.2	n.d.
K 13 (K)	f, px, [*e, c*]	5.5				4.1–6.1	0.1
K 13a (K)	f, px, ol, [*c, op, s*]				4.4	4.1–6.1	0.1
K 9 (K)	f, px, ol [*h*]	6.0	5.3		5.7, 5.8**	4.3–6.4	n.d.
K16 (K)	f, px, ol, [*c, t, op, s*]	5.3	5.1		5.2**	3.6–5.7	0.2
OM 251 (F)	f, px, ol, [*hg, c, t, s*]	6.4	5.8		6.1, 6.2**	4.7–6.8	n.d.
OM 28 (R)	f, px, ol, *a,* [*e, t, c, s*]	4.7			5.2	3.0–5.1	0.4
K 18 (K)	f, px, ol, [*a, c, s, t, e*]	4.1	4.7		4.3**	2.4–4.5	0.6
OMG 282 (D)§	h			5.4h			
			Plagiogranite (250°-400°C)				
OMG 71-2 (S)	f, q, h, *a, op,* [*c, e, p*]			4.8q	6.3	3.9–6.4	n.d.
OMG 66-3 (S)	f, [*e, sp, op,* q]				13.6	10.8–13.3	n.d.
OMG 66-1 (S)	f, h, [*op, e, p, c, a*]	8.1		5.6 (a + h)		5.8–8.1	n.d.
OMG 66-4 (S)	f, *p, c, e, op*	14.0				11.2–13.7	n.d.
OMG 64-3 (S)	f, q, *e*				9.7	6.7–9.4	n.d.
OMG 65-3 (S)	f, [q, op, *e*]			8.5q	12.4	10.0–12.5	n.d.
OMG 224-3 (K)	f, h, q, *a, c*				5.2	2.3–4.8	0.5
			Gabbro Dikes Cutting Peridotite (400°-600°C)				
KK 21a (K)	f, px, ol, [*p, s, hg, op*]	7.1	5.9			5.5–7.6	n.d.
K 21b (K)	f, px, ol, [*p, s, hg, op*]	8.2	6.0			6.6–8.7	n.d.
OMG 53 (I)	f, px, ol, [*s, hg, op*]	9.2	6.4			7.6–9.7	n.d.
C 93 (I)	f, px, ol, [*s, hg, p*]	8.1	6.3			6.5–8.6	n.d.
C 204c (I)	f, px, ol, [*s, hg, p*]	7.3	5.9			5.7–7.8	n.d.
G 141 (I)	f, px, ol, [*p, hg, s*]	7.8	6.3			6.2–8.3	n.d.

*General geographic location of samples (see Figure 1): I, Ibra; S, Wadi Saq; K, Wadi Kadir; J, Wadi Jizi; F, Wadi Fizh; R, Rustaq; D, Dasir.

†Abbreviations: h, hornblende (brown or green); a, actinolite; c, chlorite; ca, calcite; px, clinopyroxene; e, epidote; f, plagioclase; hg, hydrogarnet; l, leucoxene; ol, olivine; op, opaques; p, prehnite; pg, palagonite; q, quartz; s, serpentine; sa, saponite; sp, sphene; t, talc; z, zeolite; symbols in italics are alteration or secondary minerals; brackets enclose minor minerals (≤2% of rock).

‡Range of calculated $\delta^{18}O_{H_2O}$ in equilibrium with the rocks using the feldspar geothermometer [*O'Neil and Taylor*, 1967] and assuming a reasonable range of temperatures, based on the hydrothermal mineral assemblages (given in parentheses for each rock type).

‖ Water/rock ratios (in oxygen units) calculated from the isotopic data, using the lower-temperature limit for each rock type, and the open system equation $w/r_{open} = \ln (w/r_{closed} + 1)$ for the sheeted diabase and pillow lavas. The closed system equation (see text) was used for the gabbros and plagiogranites. Cretaceous seawater ($\delta^{18}O = -0.5$) was used for the initial H_2O. The abbreviation n.d. means that $\delta^{18}O_{H_2O}{}^{i} = -0.5$ does not yield a valid result using either the closed system or open system calculation.

§ δD values; OMG 5-3 (whole-rock = −53); OMG 71-1 (amphibole = −56); OMG 282f (hornblende = −47).

**Calculated $\delta^{18}O$ of whole-rock samples (from mineral ^{18}O data).

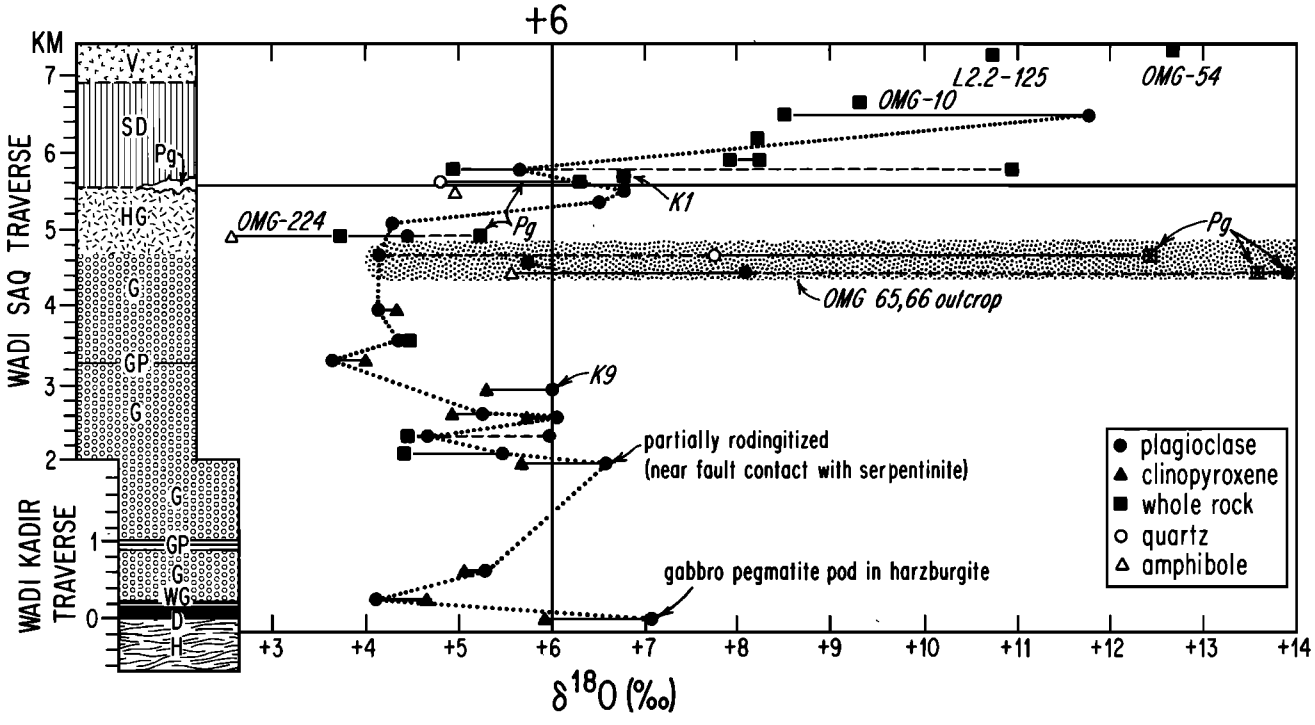

Fig. 3. Oxygen isotope data for the combined Wadi Saq and Wadi Kadir sections. Data below 2 km are from Wadi Kadir. Above 2 km the data are from Wadi Saq, except where noted by sample number. OMG 10, OMG 54, K 1, K 9, and OMG 224 are samples from the Ibra area analyzed by *McCulloch et al.* [1981]. Sample L 2.2-125 is from Wadi Jizi. Shaded area represents OMG 65 and OMG 66 outcrops, which are located at the same structural horizon in Wadi Saq. Dotted line connects analyses of plagioclase separates. Horizontal solid lines connects coexisting minerals from the same hand speciman. Horizontal dashed lines connect data points from the same outcrop but different hand specimens. Pg is plagiogranite.

pieces or calculated by material balance from the $\delta^{18}O$ values of the individual mineral phases in the assemblage. We checked our calculated whole-rock $\delta^{18}O$ values against measured values for samples K9 and OM251, and agreement was well within our experimental precision, <0.1‰.

Discussion of the Isotope Data

General Statement

The main features of the $\delta^{18}O$ data and δD data are presented graphically in Figures 3 and 4. The most striking results of this isotopic study are as follows:

1. Hydrothermal ^{18}O exchange was observed well down into the deeper levels of the cumulate gabbros and locally was found to penetrate along fractures into the upper mantle peridotites.

2. Only a few D/H results from the Oman ophiolite are reported in this study, but these are similar to the D/H data from the Troodos ophiolite [*Heaton and Sheppard,* 1977; *Magaritz and Taylor,* 1974], and they are compatible with a model of seawater-hydrothermal exchange (Figure 4).

3. A relatively systematic $^{18}O/^{16}O$ distribution was observed within the pervasively altered section, which includes all the rocks down to about 2 km above the fossil Moho (Figure 3).

4. Relative to an initial $\delta^{18}O \approx +5.7$, high-$T$ (>350°C) seawater-hydrothermal alteration produced ^{18}O-depleted rocks (down to $\delta^{18}O = +3.5$) throughout the upper cumulate gabbros, as well as locally in the lowest levels of the oceanic crustal section.

5. The ^{18}O-enriched rocks were produced in the higher levels of the oceanic crust, particularly above the contact between high-level gabbro and the sheeted diabase complex.

6. High-temperature ^{18}O exchange with hydrothermal fluids occurred at levels well below the stratigraphic horizon at which secondary hydrothermal OH-bearing minerals disappear in the cumulate gabbros.

Plagioclase-Clinopyroxene Pairs

In addition to the D/H data, evidence for deep circulation of seawater-derived hydrothermal fluids comes mainly from data on coexisting plagioclase and pyroxene. Several such mineral pairs were examined from the cumulate gabbros and gabbro dikes and veins which crosscut the peridotite. This mineral pair is particularly valuable because pyroxene is so much more resistant to hydrothermal ^{18}O exchange than is plagioclase [*Taylor,* 1968; *Taylor and Forester,* 1971; *Forester and Taylor,* 1977; *Taylor and Forester,* 1979]. Throughout the gabbro section this mineral pair exhibits oxygen isotopic disequilibrium; based on analogous results from other localities [*Forester and Taylor,* 1977; *Taylor and Forester,* 1979], it is clear that this feature is a result of subsolidus exchange.

Plagioclase-pyroxene pairs analyzed from rapidly quenched gabbroic magmas, such as terrestrial basalts and lunar microgabbros, all have $\Delta^{18}O$ plagioclase-pyroxene $\equiv \delta^{18}O$ plagioclase $- \delta^{18}O$ pyroxene ≈ 0.5, close to the equilibrium fractionation [*Taylor,* 1968; *Anderson et al.,* 1971; *Taylor and Epstein,* 1970; *Onuma et al.,* 1970]. Therefore in normal mid-ocean ridge tholeiites that have whole-rock $\delta^{18}O = 5.7$, the

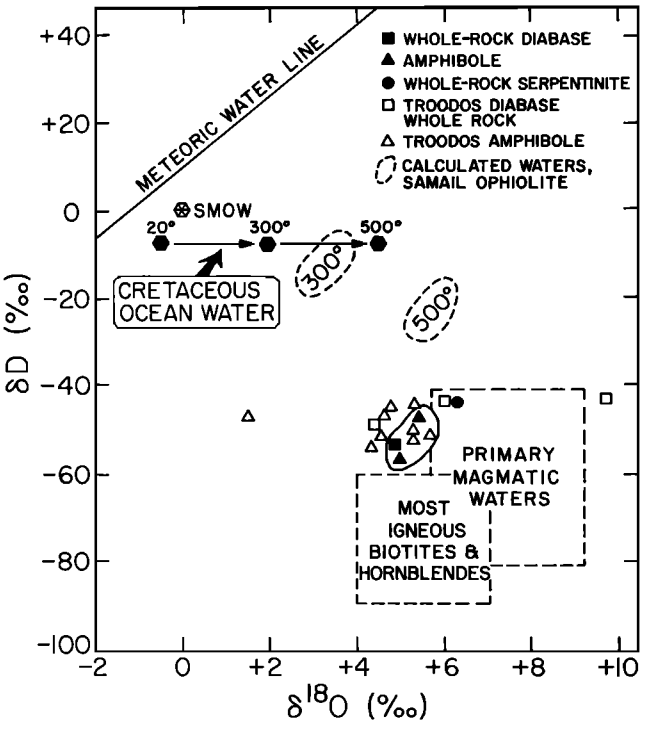

Fig. 4. Plot of δD versus $\delta^{18}O$ for rocks analyzed from the Oman ophiolite, showing calculated isotopic compositions of ^{18}O-shifted Cretaceous ocean water and of waters that would be in equilibrium with the Oman samples at $T = 300°C$ and 500°C (for details of calculation, see *Heaton and Sheppard* [1977]). Also shown for comparison are data from another Cretaceous Tethyan ophiolite, the Troodos complex, Cyprus, by *Heaton and Sheppard* [1977] and *Magaritz and Taylor* [1974].

corresponding primary magmatic $\delta^{18}O$ plagioclase should be +6.0 and the $\delta^{18}O$ pyroxene about +5.5. On a graph of $\delta^{18}O$ plagioclase versus $\delta^{18}O$ pyroxene (Figure 5), all primary magmatic plagioclase-pyroxene pairs from normal tholeiite basalts should therefore cluster around a spot having the coordinates (5.5, 6.0). If the bulk $\delta^{18}O$ value of the basaltic liquid differs from +5.7, the plagioclase-pyroxene pairs will map out a straight line of slope 1, the $\Delta = 0.5$ line on Figure 5. If the temperature of final equilibration is higher or lower than the solidus temperature of the basaltic magma, the Δ values will be smaller or larger than 0.5, respectively. All lines representing constant temperatures of equilibration of pyroxene and plagioclase on Figure 5 will have a slope of 1 and a $\delta^{18}O$ plagioclase intercept equal to $\Delta^{18}O$.

During cooling of the system plagioclase-pyroxene, $\Delta^{18}O$ will increase. Slowly cooled plutonic gabbros in fact typically exhibit plagioclase-pyroxene Δ values of 0.8 to 1.3 [*Taylor*, 1968]. From the original primary magmatic 'spot' on Figure 5, rocks undergoing closed system cooling will map out a series of points that form a right triangle whose sides are the north and west vectors emanating from the spot and whose hypotenuse is the line segment with slope = 1 that corresponds to the new temperature of final equilibration (e.g., the $\Delta = 1.5$ line segment on Figure 5). The north vector applies to cumulate layers where modal clinopyroxene ≫ plagioclase, and the west vector applies to cumulate layers where modal plagioclase ≫ clinopyroxene. All other intermediate compositions will be within the triangle. This two-component analysis works for the cumulates because the modal abundance of clinopyroxene + plagioclase is much greater than the abundance of olivine, the only other oxygen-bearing cumulus mineral.

In open systems the equilibrium plagioclase-pyroxene pairs are required to lie upon the new 'final' temperature line but not necessarily within the closed system 'triangle.' However, there are no conditions of open or closed system equilibrium cooling in which the data points can move below the primary magmatic ($\Delta = 0.5$) line on the plagioclase-pyroxene plot.

Many of the cumulate plagioclase-pyroxene pairs from the Samail ophiolite plot in the field forbidden under equilibrium conditions. In addition, the plagioclase-pyroxene pairs do not plot on an equilibrium trend with slope unity but instead plot in the vicinity of a least squares line given by the equation $\delta^{18}O$ plagioclase ≈ 2.3 $\delta^{18}O$ clinopyroxene $- 6.6$ (Figure 5). The $\Delta^{18}O$ values associated with the line of slope 2.3 include some samples that have normal igneous fractionations, and in fact, this line passes through the primary magmatic spot. As plagioclase $\delta^{18}O$ values decrease, the $\Delta^{18}O$ values decrease to zero and then become reversed. Since all equilibrium plagioclase-pyroxene $\Delta^{18}O$ values are known to be positive in the temperature range that is geologically reasonable ($T < 1300°C$), the trend of data points in Figure 5 constitutes clear-cut evidence for open system (hydrothermal) subsolidus exchange. The plagioclase-pyroxene graph is a very sensitive indicator of subsolidus disequilibrium exchange, as well as testing for open or closed system conditions. Figure 5 shows that virtually all of the plagioclase-pyroxene pairs in the Samail gabbro have exchanged under open system conditions.

Trend lines similar to the one illustrated in Figure 5 have been reported for the Skaergaard intrusion and the Cuillin

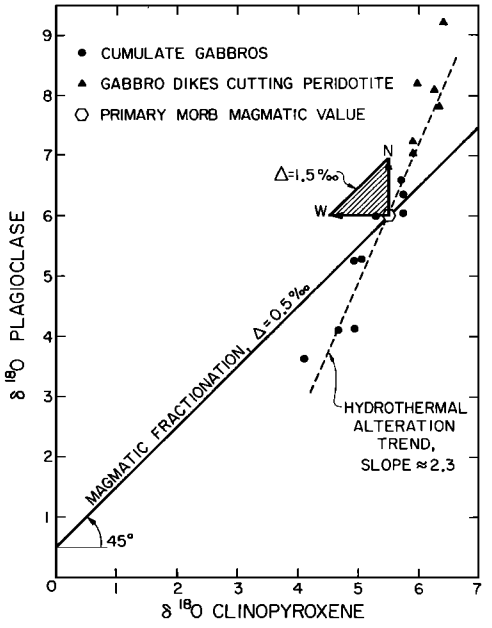

Fig. 5. Plot of $\delta^{18}O$ plagioclase versus $\delta^{18}O$ clinopyroxene for samples from the cumulate gabbro and from gabbro dikes in the peridotite. These data plot on trends forbidden during closed system equilibrium cooling (see text).

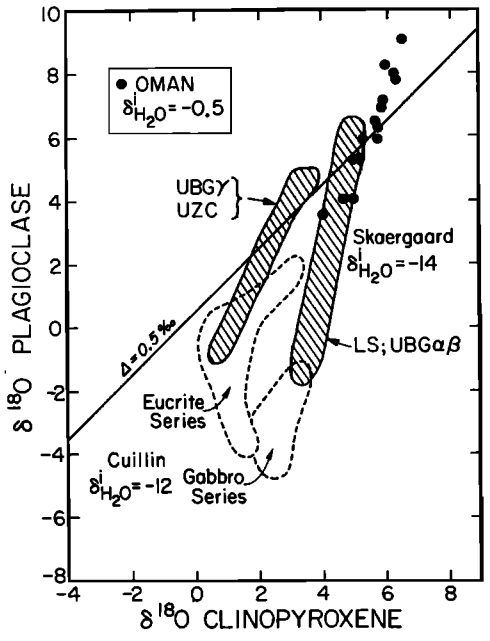

Fig. 6. Comparison of $\delta^{18}O$ data on clinopyroxene-plagioclase pairs from Oman (solid circles) with analogous data from the Skaergaard (hatched pattern; UBG is Upper Border Group; LS is Layered Series; UZc is Upper Zone C of the Layered Series) and Cuillin gabbros (dashed envelopes); the latter were altered by meteoric-hydrothermal fluids [*Taylor and Forester,* 1979; *Forester and Taylor,* 1977]. The Oman data form a more systematic, narrower band which possibly indicates less closed system, subsolidus cooling prior to interaction with hydrothermal fluids. This may reflect the more tectonically active spreading regime for the ophiolite rocks. The $\Delta = 0.5$ line (45°) represents the accepted ^{18}O fractionation between pyroxene and plagioclase at magmatic temperatures [*Anderson et al.,* 1971].

gabbro of the Isle of Skye [*Forester and Taylor,* 1977; *Taylor and Forester,* 1979]. As shown in Figure 6, the slopes of these meteoric-hydrothermal alteration trajectories vary from approximately two to four. These differences in slope are suggestive of differing exchange rates between the various clinopyroxenes and aqueous solutions. Some of the obvious factors that will influence the slope of the alteration trend are grain size, degree of exsolution, fluid-phase composition, $\delta^{18}O$ of the fluid, and perhaps equilibration time. The cumulate plagioclase-pyroxene pairs in Oman display a slope that is less steep than that shown by most of the Skaergaard samples, although they do trend parallel to the UBG, UZc, and Sandwich Horizon pairs from the Skaergaard intrusion, where the effective grain size of the clinopyroxene has been significantly reduced by subsolidus recrystallization and inversion from a β wollastonite precursor [*Taylor and Forester,* 1979]. Inasmuch as the Oman clinopyroxenes exhibit exsolution features and grain sizes comparable to the rest of the Skaergaard Layered Series, where the alteration slope is approximately four, this raises the question as to which of the other parameters listed above is controlling the slopes.

Let us assume that at a given T, clinopyroxene exchanges with a hydrothermal fluid at a fixed (slower) rate than does plagioclase. This is essentially identical to stating that the effective water/mineral ratio is lower for pyroxene than for plagioclase (i.e., the pyroxene 'sees' less H_2O than the adjacent coexisting plagioclase). By setting the water/mineral ratio for plagioclase (An_{75} for the cumulates) equal to a constant times the water/mineral ratio for clinopyroxene, $\delta^{18}O$ trajectories of the plagioclase-pyroxene pairs from the Oman ophiolite and the Skaergaard intrusion can be simulated (Figure 7). In this illustration the initial Oman $\delta^{18}O_{H_2O}$ is assumed to be −0.5, and the 'initial' Skaergaard $\delta^{18}O_{H_2O} \approx -5.0$ [*Norton and Taylor,* 1979]. This initial Skaergaard fluid composition is an ^{18}O-shifted surface water which originally had a $\delta^{18}O_{H_2O} \approx -14.0$ based on D/H systematics [*Taylor and Forester,* 1979]. The boundaries of the fields on Figure 7 are defined arbitrarily by assuming a 500°C exchange temperature, and rate constants for plagioclase that are a factor of 2–5 times faster than for pyroxene.

The plotted curves bracket the actual data from both the Skaergaard and Oman and suggest the plagioclases exchanged between 3 and 5 times more rapidly than the coexisting pyroxenes (near the 5× curves on Figure 7). The different slopes, two and four, respectively, for Oman and the Skaergaard are a consequence of the drastically different $\delta^{18}O$ compositions of the hydrothermal fluids. For most mineral-water systems the first derivative of the hydrothermal exchange curve will equal the rate constant, if small (open system) water/rock ratios prevail. The larger the difference between initial fluid and initial rock, the more closely will the measured points reflect the rate constant. A second implication of Figure 7 is that the Skaergaard Layered Series and the Samail gabbros both achieved approximately the same water/rock ratio ≈ 0.15 (open system mass units). This relatively crude estimate of the water/rock ratio is actually very close to the value (≈0.20 for the layered series) calculated by *Norton and Taylor* [1979] in a much more complete numerical modeling study of the Skaergaard intrusion. This suggests that many of the important parameters, such as permeability, porosity, etc., used by *Norton and Taylor* [1979] in their analysis of the Skaergaard gabbro also would apply to the Samail gabbro and thus to the oceanic crust in general.

The above discussion indicates that the most important factors in fixing the final $\delta^{18}O$ values of mineral pairs affected by hydrothermal alteration are (1) initial $\delta^{18}O_{H_2O}$, (2) amount of fluid flushed through the system, (3) average temperature of exchange, and (4) grain size (especially when intense grain-boundary recrystallization or mineral exsolution occurs). Salinity differences in the aqueous fluids appear to be less important, at least at concentrations lower than that exhibited by normal seawater.

Isotopic Changes in the Hydrothermal Fluids

Meteoric-hydrothermal systems associated with the continental intrusions described above (initial $\delta^{18}O_{H_2O} \approx -9$ to −14) invariably result in ^{18}O depletions of the rocks and minerals, whereas in the Samail ophiolite the hydrothermal interaction has produced both ^{18}O depletions and ^{18}O enrichments. This is because the $\delta^{18}O$ of Cretaceous seawater ($\delta^{18}O_{H_2O} \approx -0.1$ to −0.7; see below) is only about 6‰ lower than that of the initial igneous rock instead of 15–20‰ lower, as in the subaerial examples. Changes in both temperature and water/rock (w/r) ratio (leading to ^{18}O shifts in the hydrothermal fluid) can result in the observed ^{18}O shifts in the rock either up or down.

Let us consider the plagioclase-water system, whose $\Delta^{18}O$ is given by

$$\Delta^{18}O_{\text{plagioclase-}H_2O} = \frac{2.91 - 0.76\beta}{T^2} \times 10^6 - 3.41 - 0.14\beta$$

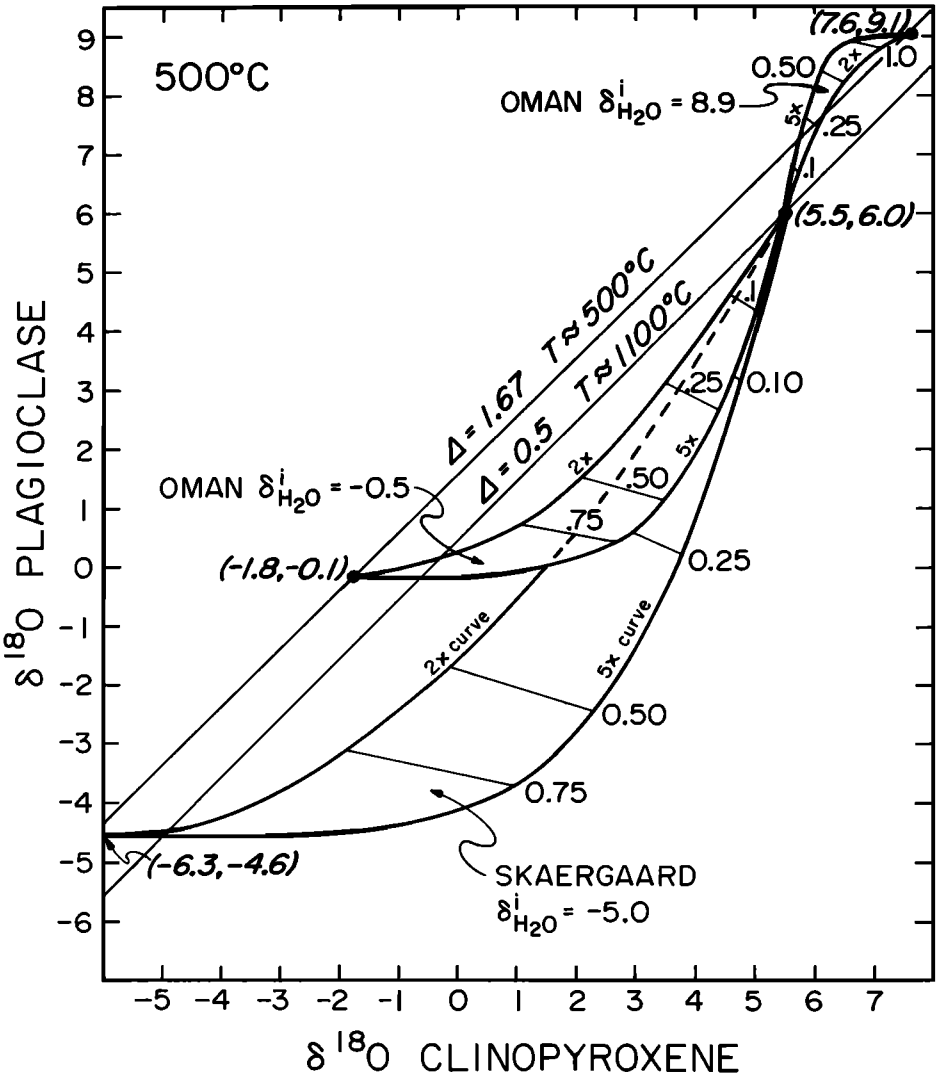

Fig. 7. Plot of $\delta^{18}O$ plagioclase (An_{75} cumulates; An_{90} gabbros in the peridotite) versus $\delta^{18}O$ clinopyroxene for the Oman and Skaergaard mineral-pair trajectories. The curves are calculated in two ways: (1) analytically by setting $(w/r)^{\text{plagioclase}}_{\text{open system}} = K \times (w/r)^{\text{clinopyroxene}}_{\text{open system}}$ or (2) by a finite element technique which allows small but different (by a constant factor) increments of water to equilibrate with plagioclase and as the integrated w/r ratio builds up with each step. Both methods yield the same curves. These paths represent cooling, accompanied by hydrothermal exchange, starting at the magmatic coordinates (5.5, 6.0; $\Delta = 0.5$) and proceeding to $T \approx 500°C$ ($\Delta = 1.67$). The initial $\delta^{18}O_{H_2O}$ is assumed to be −5.0 at Skaergaard [*Norton and Taylor*, 1979] and either −0.5 or +8.9 at Oman; the former value is Cretaceous seawater, and the latter value represents magmatic water or strongly ^{18}O-shifted seawater in the deepest parts of the Samail hydrothermal system. Two calculated curves are shown, arbitrarily assuming that plagioclase exchanges with H_2O at a rate either 2 times (2×) or 5 times (5×) faster than clinopyroxene. Water/rock ratios of 0.1, 0.25, 0.50, 0.75, and 1.0 (in weight units) are represented by tie lines connecting the 2× and 5× curves, assuming the rock contains 60% plagioclase and 40% clinopyroxene. The intersection of the exchange curves with the $\Delta = 1.67$ line corresponds to an infinite water/rock ratio. The cumulate gabbro trajectories mimic the behavior of the $\delta^{18}O$ values of actual mineral assemblages shown in Figure 6, in that the latter do indeed plot on the high-temperature side of the magmatic isotherm ($T \approx 1100°C$).

where β is anorthite content of the plagioclase and T is in °K [*O'Neil and Taylor*, 1967]. If a packet of seawater with $\delta^{18}O = 0$ equilibrates with cumulate plagioclase (An_{80}, $\delta^{18}O = +6$) at 800°C, the water will approach a $\delta^{18}O$ value of +7.5. If this strongly ^{18}O-shifted H_2O packet then moves up section and exchanges with plagioclase in the sheeted diabase complex at 350°C, then the feldspar $\delta^{18}O$ value will increase to +10 ($w/r \gg 1$) or +8 ($w/r \approx 1$). If we further lower the temperature of alteration in the diabase, the $\delta^{18}O$ of this plagioclase will become even higher. For example, at 200°C the $\delta^{18}O$ of the feldspar would be about +14 ($w/r \gg 1$) or +10 ($w/r \approx 1$). Inasmuch as the upper level feldspars are typically more Na rich than An_{80}, the final $\delta^{18}O$ values will actually be even higher (for pure albite, +12 to +9 and +17 to +12, respectively, at 350°C and 200°C).

The final $\delta^{18}O$ of any small volume of rock in the ophiolite will depend strongly upon the previous exchange history or path of the water packets with which it interacts. In a zone where stream lines of fluid circulation are concentrated, as is likely in the sheeted dike complex near the distal edge of the

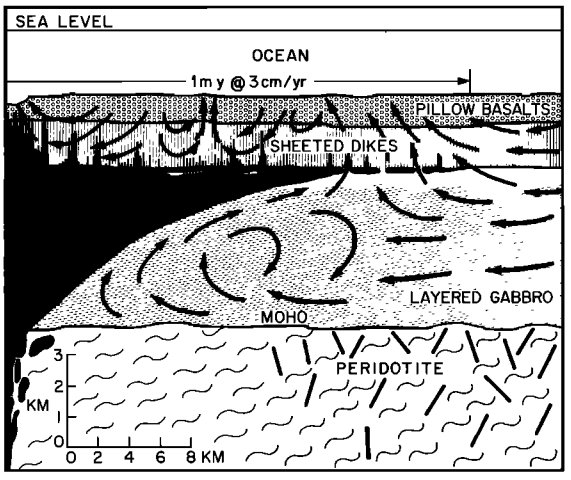

Fig. 8. Cartoon sketch showing probable seawater circulation patterns in a cross section of the Samail ophiolite at the time of its formation. The solid black indicates magma. Note the existence of two essentially isolated circulation regimes, separated by a thin sheet of magma that is essentially impermeable to the fluids in the hydrostatic convective system. One system (the upper system) extends outward from the ridge axis and is located directly over the magma chamber, and the other (the lower system) lies underneath the wings of the magma chamber. The two systems interact with one another only at the distal edges of the magma chamber. Also shown is the lateral distance that would be traversed by this oceanic crustal section in 1 m.y., assuming a half spreading rate of 3 cm/yr. The high-level noncumulate gabbro is shown as a blank pattern between the sheeted dikes and the layered gabbro. The wavy line pattern in the peridotite represents the tectonite fabric, and the short heavy lines schematically indicate gabbro dikes filling conjugate fractures that postdate the tectonite fabric; locally, the hydrothermal circulation penetrated these conduits. Note that only one side of the MOR spreading system is illustrated; a mirror image of the above diagram should exist to the left side of the figure.

magma chamber (see Figure 8), arguments such as those given above would predict ^{18}O enrichments in the rocks. In addition, plagioclase is likely to continue to exchange down to temperatures at least as low as 150°–200°C as long as it is in contact with hydrothermal fluids. The combination of these processes probably explains the apparent inconsistency between diabase dikes with $\delta^{18}O_{plagioclase} = 11.8$ and mineral assemblages suggesting $T = 300°–350°C$ (i.e., sample OMG 10). It is clear from this analysis that the hydrothermal fluids in the ophiolite all were strongly modified by exchange and that none could be considered to be pristine seawater. Assuming plausible temperatures of equilibration for the plagioclase and whole-rock samples given in Table 1, the calculated equilibrium $\delta^{18}O_{H_2O}$ values range from −3 to +10.

Gabbro dikes which postdate the peridotite tectonite fabric probably represent crystallization products of melts moving through the peridotite [*Boudier and Coleman*, 1981]. These dikes line conjugate fracture sets in the tectonites or occur as local segregations near plagioclase-bearing peridotite. Plagioclase-pyroxene pairs from these gabbros have $\delta^{18}O$ values which plot on the high-^{18}O extension of the disequilibrium least squares trend line mapped out for the gabbros (Figure 5). For these dike samples it is important to note that the isotopic analyses were performed upon mineral separates purified to a high degree with heavy liquids to avoid any high-^{18}O rodingite minerals. Even though petrographically unaltered plagioclase and pyroxene were analyzed, the exchange trend extends to approximately a 300°–400°C isotherm, suggesting the exchange mechanism was similar to that found in the ^{18}O-depleted gabbros higher in the ophiolite section.

A plausible explanation for the high $\delta^{18}O$ values of these dikes and veins is that because they are the deepest samples, the hydrothermal fluids had previously exchanged with very large amounts of overlying oceanic crustal and/or upper mantle rocks at relatively high temperatures. Thus these small amounts of deeply circulating H_2O would have become strongly enriched in ^{18}O as they moved down into fractures in the peridotite. Inasmuch as these conjugate dikes postdate the tectonite fabric, their formation and subsequent alteration also must have occurred at a temperature lower than that of the high-temperature regime [*Nicolas et al.*, 1980] in which the tectonite fabric was formed. As the rocks moved away from the ridge axis, the plagioclase-pyroxene pairs in the dikes would have continued to exchange at successively lower temperatures, which may also in part account for the high $\delta^{18}O$ values. The ^{18}O effects are most strongly developed in the dikes and veins because at any given stratigraphic horizon the water/rock ratios would be expected to be highest along the fractures which are acting as hydrothermal conduits. It is, in fact, very common in plutonic igneous complexes to find unusually large ^{18}O effects in dikes and along fractures [*Forester and Taylor*, 1977; *Taylor and Forester*, 1979; *Magaritz and Taylor*, 1976*b*].

In Figure 7 the plagioclase-clinopyroxene trajectories for $T = 500°C$ are plotted for a water that had been ^{18}O shifted to $\delta^{18}O = 8.9$, which implies that this water equilibrated with a large amount of gabbro or upper mantle olivine and pyroxene. The trajectories show that exchange with such an ^{18}O-shifted water at temperatures of the order of 500°C is a plausible explanation for the high-^{18}O plagioclase and pyroxene. However, ^{18}O-shifted seawater of +8 composition is essentially indistinguishable in its $\delta^{18}O$ value from magmatic water, so the latter also must be at least considered as a plausible candidate. Possibly, $^{87}Sr/^{86}Sr$ or D/H studies might help distinguish between magmatic H_2O and ^{18}O-shifted seawater, but no secondary, high-temperature, hydrous minerals are available in these samples, and if the oxygen had shifted to +8, then the Sr isotopes would also probably be buffered by exchange with the rocks. An additional complication is that any late stage, exsolved magmatic water with $\delta^{18}O \approx +8$ could represent H_2O originally driven into the melt by dehydration of hydrothermally altered stoped blocks of roof rock [*Gregory and Taylor*, 1979; *Taylor*, 1980]. However, neither this type of magmatic water nor a primary magmatic water is deemed to be likely candidates, because the gabbro dikes and veins predominantly occur in conjugate sets which postdate the peridotite tectonite fabric. This in turn suggests that the alteration probably occurred well out on the flanks of the ridge, where ^{18}O-shifted seawater would be the most likely type of hydrothermal fluid (Figure 8).

$\delta^{18}O$ Variations in the Ophiolite Sequence

A few cumulate gabbro samples have been found that have apparently closely preserved their magmatic $\delta^{18}O$ values (samples K 9, OMG 67). As might be expected, these are most common in the lower section of cumulates. However, particularly in the vicinity of fractures and prominent veins containing high-T mineral assemblages, low-^{18}O gabbros have been found at very great depths, for example, within 250 m of the tectonite peridotite-gabbro contact. Approximately 2 km

above the base of the cumulates, plagioclase $\delta^{18}O$ values decrease to a minimum of 3.6 in the Wadi Saq section (Figure 3). Coexisting pyroxene in this sample has $\delta^{18}O$ equal to 4.1.

Mineralogical evidence for alteration is practically nonexistent in all these lower cumulates, even those that are markedly depleted in ^{18}O. Thin reaction rims of talc + magnetite around olivine grains occur locally in the low-^{18}O rocks but are not universal. Plagioclase generally appears to be completely unaltered. Pyroxenes, although generally unaltered, may contain minor (<10%) replacement brown amphibole along grain cleavages and fractures. These data indicate that the hydrothermal alteration of most of the gabbro samples occurred at extremely high temperatures and that subsequently, there was only local influx and exchange with low-T waters.

One of the samples studied by *McCulloch et al.* [1981] is K 9, in which $\delta^{18}O$ plagioclase = 6.0 and $\delta^{18}O$ clinopyroxene = 5.3; during cooling, this sample suffered very little exchange, and also it apparently behaved essentially as a closed system in terms of its oxygen. The plagioclase $\delta^{18}O$ value has remained almost constant, compatible with its large modal abundance (75%) in this specimen. The initial $^{87}Sr/^{86}Sr$ value of the plagioclase also has been almost unaffected, although the $^{87}Sr/^{86}Sr$ of the clinopyroxene was slightly increased, compatible with its lower modal abundance and lower Sr content [*McCulloch et al.*, 1981]. This clinopyroxene also shows a slight overgrowth of brown amphibole, always in optical continuity in each grain. The strontium isotope data demonstrate that small amounts of heated seawater have affected this sample during subsolidus cooling, and together with the ^{18}O data this suggests that the amphibole in K 9 grew at temperatures just below the solidus in communication with small amounts of strongly ^{18}O-shifted, seawater-derived hydrothermal fluid ($\delta^{18}O_{H_2O} \approx +8.1$, $^{87}Sr/^{86}Sr \approx 0.7044$).

The various isotopic relationships in K 9 were all established, or 'frozen in,' at high temperatures, and virtually no exchange occurred at extremely low temperatures. Similar statements can be made about all of the cumulate gabbros, most of which were much more strongly hydrothermally altered at high T than was K 9. The lack of low-temperature retrograde alteration is evidenced by the 'unaltered' plagioclase, the unaltered or only slightly amphibolitized clinopyroxene, the absence of serpentine alteration of olivine, and the presence of only minor talc + magnetite. In all these samples the alteration and oxygen exchange must have occurred at temperatures exceeding 400°C, with most exchange probably at much higher temperatures. As the temperature dropped below about 300°C, the water/rock ratio in the main mass of cumulates must have dropped to a value very near zero, except in the immediate vicinity of the vein and fracture systems. The process described above is well documented in many continental gabbro bodies [*Taylor*, 1971; *Forester and Taylor*, 1977; *Taylor and Forester*, 1979; *Taylor and Coleman*, 1977], which also were altered at very high temperatures and which exhibit a paucity of OH-bearing hydrothermal minerals. For example, by numerically modeling the Skaergaard hydrothermal system, *Norton and Taylor* [1979] showed that more than half of the H_2O that was ultimately 'pumped' through this gabbro body went through at $T > 480$°C, with maximum fluid flux at around 600°C.

Above the minimum ^{18}O stratigraphic horizon in the cumulate gabbros the $\delta^{18}O$ values tend to systematically increase upward. These upper cumulates are indistinguishable in hand specimen and in thin section from the low-^{18}O lower cumulates. In conjunction with this enrichment in ^{18}O, as the gradational contact between the cumulate gabbro and high-level gabbro is approached, OH-bearing alteration minerals become more abundant. Brown amphibole is followed by green amphibole, then chlorite appears, and finally in some rocks, rare epidote occurs in the high-level gabbros. The presence of talc + magnetite after olivine (and the lack of serpentine or chlorite) in some high-level gabbros again demonstrates that most of the hydrothermal fluids were flushed through at temperatures exceeding 400°C. The $\delta^{18}O$ plagioclase varies from 4.5 to 6.8, generally increasing upward in the high-level gabbros. Whole-rock $\delta^{18}O$ values of the high-level gabbros vary from 3.7 to 6.8 and may coincidentally approximate normal igneous values. Although absent from meteoric-hydrothermal systems, this 'coincidence' phenomenon is a characteristic feature of seawater-hydrothermal systems. Because of the ^{18}O shifts and the relatively high initial $\delta^{18}O$ value of the ocean water, there is a significant range of temperatures over which the whole-rock $\delta^{18}O$ value of a gabbro that has been thoroughly hydrothermally altered in the presence of large amounts of water will, simply by coincidence, be very close to the primary magmatic value of +5.7.

Above the sheeted diabase-gabbro contact, actinolite, chlorite, saussurite, leucoxene, and epidote all become common in the alteration mineral assemblages. Amphibolite facies assemblages give way rapidly up section to greenschist assemblages. Feldspar separated from diabase OMG 5c located less than 200 m above the gabbro contact had a $\delta^{18}O = 5.2$, while OMG 10 diabase approximately 300 m below the pillow lava contact has a $\delta^{18}O$ plagioclase = 11.8. The whole-rock $\delta^{18}O$ values are +4.9 and +8.5, respectively. Pillow lava OMG 54 has $\delta^{18}O$ = 12.9 and contains plagioclase (An_{25}), palagonitized glass, abundant zeolites, and secondary carbonate. Piecing the two stratigraphic columns together, the $\delta^{18}O$ values of whole-rock samples decrease from about +13 in the pillow lavas down to values which approximate normal igneous rocks near the gabbro-sheeted diabase contact. Further down section, $\delta^{18}O$ continues to decrease to a minimum value approximately 1.5 to 2 km below the diabase-gabbro contact. After passing through a minimum value of about 3.8 the whole-rock $\delta^{18}O$ values again tend to increase sporadically down section through to the lowermost gabbros, where the exchange effects are localized along fractures and veins.

Neither Wadi Kadir or Wadi Saq represent complete sections through the ophiolite, but where they overlap, the agreement between geology, petrography, alteration mineralogy, and the $\delta^{18}O$ profile is very good. The consistency of geology and $\delta^{18}O$ profiles in these two sections separated by a lateral distance of over 15 km, as well as the basically similar geologic sections exposed over several hundred kilometers of the entire Oman mountain belt, both suggest that we are looking at a representative cross section through the Tethyan oceanic crust. It also appears that the physical and chemical processes involved in formation of this oceanic crust had essentially reached steady state conditions, in the 5- to 10-m.y. interval after igneous crystallization and before detachment. This steady state crustal section contains significant volumes of both low-^{18}O (<+6) plutonic rocks and high-^{18}O (>+6) hypabyssal and pillowed volcanic rocks. The upper parts of this mature piece of oceanic crust at Ibra also appear to be very similar to, and representative of, many other ophiolites in terms of both alteration history and $\delta^{18}O$ values [*Heaton and*

Sheppard, 1977; *Magaritz and Taylor,* 1974; 1976*a*; *Williams and Malpas,* 1976; *Gregory,* 1980; *Stern et al.,* 1976].

Isotopic Aging of the Oceanic Crust

The range of whole-rock $\delta^{18}O$ values of diabase dikes from the Wadi Saq and Wadi Kadir sections is +6.8 to +10.9 (one sample of a late, highly chloritized dike has $\delta^{18}O$ = +4.9). However, the range of whole-rock $\delta^{18}O$ values in diabasic xenoliths (now hornfels) associated with plagiogranites from the Dasir area (about 70 km NW of Ibra, see Figure 1) is +3.7 to +6.3 [*Gregory and Taylor,* 1979]. The Dasir xenoliths represent fragments of diabase dikes from the roof of the gabbro magma chamber that became incorporated into the magma by piecemeal stoping and foundering of the roof.

The stoped blocks at Dasir record a different, earlier stage of hydrothermal alteration than does the Ibra diabase section. The Dasir xenoliths in part preserved the low $\delta^{18}O$ values that they had attained just prior to their being stoped into the underlying magma near the ridge axis. In contrast, although the lower parts of the Ibra diabase section probably also underwent a similar high-*T*, ^{18}O depletion, they did not preserve these low $\delta^{18}O$ values when they were later subjected to interaction with more ^{18}O-shifted, lower-temperature hydrothermal fluids in the vicinity of the distal portions of the magma chamber as the oceanic crust migrated away from the ridge axis (see Figure 8). The difference in ^{18}O contents can be attributed to the different circulation systems, temperatures, and types of fluid that the two suites of diabases experienced.

The xenolith suite was altered directly above and virtually in contact with the magma chamber in a region where the hydrothermal circulation system was dominated by high-temperature fluids that circulated to depths of only 2–3 km and interacted only with basalt and diabase. Because of the high water/rock ratios (see below and *McCulloch et al.* [1981]), this fluid would not have suffered any large ^{18}O shifts and thus would be isotopically similar to seawater; the fluid path lines would not take it through the lower portions of the oceanic crust. However, as the crust continues to spread, the diabase section moves beyond the distal edge of the magma chamber (Figure 8) into a regime where the fluids are dominantly moving upward from deep in the cumulate gabbro section. Such fluids may still be at relatively high temperatures, but because of overall lower water/rock ratios in the less permeable, deeper parts of the ocean crust, they will have suffered much more dramatic ^{18}O shifts because of interactions with the lower cumulates. During continued spreading, the temperatures also continue to decrease, which also leads to ^{18}O enrichment of the altered rocks. When the high-^{18}O and/or low-*T* fluids interact with the sheeted diabase complex, it becomes enriched in ^{18}O, thus partly masking the earlier low-^{18}O exchange history. Another factor probably involved in the preservation of the low $\delta^{18}O$ values of the Dasir xenoliths is the fact that they were carried down to deeper levels; they now lie approximately 200 m below the diabase-gabbro contact, where they are associated with large masses of plagiogranite.

This type of isotopic aging described above can also be seen on the scale of an individual outcrop. Samples from localities OMG 65 and OMG 66 (see Figure 3) in Wadi Saq exhibit the same general type of time-$\delta^{18}O$ trends. Samples from the host rock cumulate gabbros have $\delta^{18}O$ plagioclase = 4.2 to 5.8, whereas the later hornblende-gabbro segregations have $\delta^{18}O$ plagioclase = 8.1, and the still later plagiogranite dikes and veins have $\delta^{18}O$ whole rock = 12.4 to 13.6. The high-^{18}O plagiogranites occupy a prominent fracture system and have sharp nonchilled contacts against the host gabbros. In these fracture systems the fluids continued to circulate down to relatively low temperatures (as recorded by plagioclase turbidity and the presence of prehnite, epidote, and thullite). The coarser grained host gabbros have partially preserved their earlier formed lower ^{18}O values, and they also contain only amphibole as a new alteration phase (they have no epidote). The pegmatitic segregations of hornblende gabbro almost certainly crystallized in the presence of an aqueous fluid phase, but inasmuch as these segregations predate the plagiogranites, this was a different, earlier stage hydrothermal fluid than that which affected the plagiogranite. Thus in this single OMG 65, 66 outcrop we can observe practically the entire range of $\delta^{18}O$ values in the Samail ophiolite, simply by sampling the host rocks as well as the later rock types that occupy the vein and fracture systems.

IMPLICATIONS FOR THE ISOTOPIC HISTORY OF THE OCEANS

Average $\delta^{18}O$ Value of a Section Through the Oceanic Crust

The completeness of the Ibra section, together with the consistency of the geology and the relative simplicity of the mineralogic and isotopic alteration patterns, makes the Samail ophiolite an ideal place to calculate the average $\delta^{18}O$ value of mature, altered oceanic crust. For this purpose we have combined the Wadi Kadir and Wadi Saq sections. Inasmuch as the pillow lavas are not very well represented in the Ibra section, we also have added analyses of three samples from Wadi Jizi, where pillowed volcanic rocks are abundant. All these data are plotted on Figure 9. For a few of the coarser-grained gabbro samples the whole-rock $\delta^{18}O$ values plotted on Figure 9 were calculated by material balance from the modes and the mineral $\delta^{18}O$ values.

The pillow lavas ($\delta^{18}O$ = +12.7 at Ibra; +10.7 to +12.5 at Wadi Jizi) are the most poorly characterized portion of the Ibra section, but this is also volumetrically the smallest unit (<10% of the total column) and thus the least critical in the overall material balance calculation. Also, it should be noted that many pillow lavas have been analyzed from other ophiolites and they consistently define a range of about +10 to +14 [*Heaton and Sheppard,* 1977; *Magaritz and Taylor,* 1976*a*; *Spooner et al.,* 1974].

When a $\delta^{18}O$ integration (material balance calculation) is done for the entire Ibra section, it is seen that the contribution of ^{18}O-depleted rocks in the lower sequence does indeed almost exactly cancel out the contribution of the ^{18}O-enriched rocks in the upper sequence, thus strongly supporting the Muehlenbachs-Clayton hypothesis (Figure 9). The net change in ^{18}O content of the entire oceanic crust produced by the long history of hydrothermal alteration and isotopic aging of the Ibra section appears to be essentially zero. Our calculated average $\delta^{18}O = 5.8 \pm 0.3$ is, within experimental and geologic error, identical to the average $\delta^{18}O$ of MOR basalts (+5.7), which is accepted to be the primary magmatic $^{18}O/^{16}O$ ratio of the oceanic crust, as well as the overall earth-moon system [*Muehlenbachs and Clayton,* 1972*a*; *Taylor,* 1968; *Taylor and Epstein,* 1970].

If there has been no net change in $\delta^{18}O$ of the oceanic crust, there obviously cannot have been any net ^{18}O flux either into or out of seawater as a result of interactions at MOR spread-

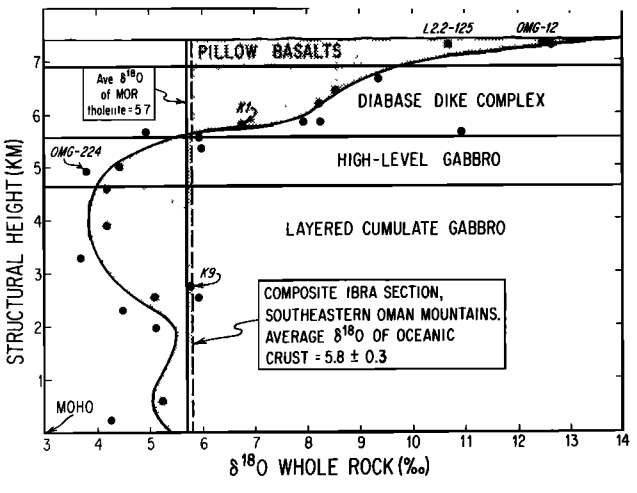

Fig. 9. Material balance calculation for the generalized $\delta^{18}O$ profile displayed by the Ibra section (solid curve fitted to the data by inspection), based on the combined Wadi Saq and Wadi Kadir traverses. Data points are all whole-rock values; samples exhibiting anomalous $\delta^{18}O$ at a single outcrop such as plagiogranite dikes and hornblende pegmatite segregations cutting massive gabbro (OMG 65, 66) and samples adjacent to veins are volumetrically insignificant and thus were not used in this calculation. Samples from Wadi Kadir that lie above the 2-km level are labeled and added to the diagram approximately at their correct stratigraphic positions, assuming that the gabbro sections were initially the same thickness, measuring downward from the diabase-gabbro contact. The stippled areas shown on the diagram are equal in size, and the average $\delta^{18}O$ of this section of altered oceanic crust is 5.8 ± 0.3.

ing centers. If we extrapolate the relationship discovered in the Samail ophiolite to all oceanic spreading centers, it is clear that seawater must have been in steady state isotopic balance, with a $\delta^{18}O$ close to zero during the Cretaceous. However, it is instructive to inquire in more detail exactly what was the buffered $\delta^{18}O$ value of Cretaceous seawater? The overall average steady state $\Delta^{18}O$ fractionation between oceanic crust and seawater is defined as $\Delta = +5.7 - \delta^{18}O_{SW}$, where $\delta^{18}O_{SW}$ is the buffered value of (Cretaceous) seawater.

The exact $\delta^{18}O$ value of Cretaceous seawater is not known, but we can place certain limits upon it. The Cretaceous is widely thought to represent a time period when there was little or no continental glaciation on earth [*Steiner and Grillman*, 1973]. We know that rapid melting of all of the present-day ice sheets, which have an average $\delta^{18}O$ of about −35, would only lower the $\delta^{18}O$ value of seawater by about 0.3 to 0.9‰ [*Dansgaard and Tauber*, 1969], and certainly by no more than 1.5‰. However, because of the cycling of seawater through the oceanic crust, it is obvious that we cannot calculate the $\delta^{18}O$ of Cretaceous seawater in this simple fashion, as the following discussion will demonstrate.

Calculation of $^{18}O/^{16}O$ Mass Balance During Cycling of Seawater Through the Oceanic Crust

Inasmuch as we are only concerned with ^{18}O balance, in the following discussion all mass units or amounts are given in grams of oxygen:

- W mass of the oceans;
- R spreading rate in km²/yr, roughly equivalent to half spreading rates in cm/yr for the present-day mid-ocean ridge systems;
- cR mass of oceanic crust created and matured each year (eventually almost all of this is subducted); c is a constant determined by the depth of exchange in the oceanic crust and by the need to convert spreading rates to grams of oxygen;
- w total amount of water that circulates through and exchanges with the oceanic crust to achieve maturity, equal to $\int_0^{t_m} \bar{w}\, dt$, where $\bar{w}$ is the average amount of water circulated per unit time and t_m is the time taken to reach maturity or a steady state profile;
- r total amount of new oceanic crust that exchanged with w amount of seawater, equal to $\int_0^{t_m} \bar{r}\, dt$, where $\bar{r}$ is the amount of rock exchanged with w per unit time; if unit time is expressed in years, $\bar{r} = cR$;
- ϕ equal to w/r; actual water/rock ratio in oxygen units for the ridge system;
- δW $\delta^{18}O$ of the oceans (assumed to be well mixed);
- $\delta_{\text{rock final}}$ final average $\delta^{18}O$ of the mature oceanic crust as it is subducted, equal to δ_{rf};
- $\delta_{\text{rock initial}} = \delta_{ri} = +5.7 = \delta^{18}O_{\text{MORB}}$;
- $\delta_{\text{water final}}$ $\delta^{18}O$ value of water that has actually circulated through the oceanic crust and discharged back into the oceans, neglecting H_2O added to the crust by hydration reactions, equal to δ_{wf};
- $\Delta^{18}O_{\text{crust-seawater}} = \delta r_i - \delta^{18}O_{SW}$ (steady state) $\equiv \Delta$.

Assuming conservation of mass, one may readily derive the following expression which relates the change in ^{18}O content of the oceans to the amount of water circulated through the oceanic spreading centers and to the ^{18}O change in that fluid as a result of its exchange with the oceanic crust:

$$W\, d(\delta W) = (\delta_{wf} - \delta W)\, dw = -(\delta_{rf} - \delta_{ri})\bar{r}\, dt \qquad (1)$$

Using the closed system water-rock equation [*Taylor*, 1971], we can solve for δ_{wf}:

$$w/r = \phi = \frac{\delta_{rf} - \delta_{ri}}{\delta W - \delta_{wf}} \qquad \delta_{rf} = \Delta + \delta_{wf}$$

$$\delta_{wf} = \frac{\phi\ \delta W - \Delta + \delta_{ri}}{\phi + 1} \qquad \delta_{rf} = \frac{\phi \delta W + \phi\Delta + \delta_{ri}}{\phi + 1} \qquad (2)$$

By substitution, (1) becomes

$$W\, d(\delta W) = \frac{-\Delta + \delta_{ri} - \delta W}{\phi + 1}\, dw = \frac{\phi(-\Delta + \delta_{ri} - \delta W)\, \bar{r}\, dt}{\phi + 1} \qquad (3)$$

Rearranging terms,

$$\frac{d(\delta W)}{\delta W + \Delta - \delta_{ri}} = -\frac{dw}{W(\phi + 1)} = -\frac{\phi \bar{r}\, dt}{W(\phi + 1)} \qquad (4)$$

Integration of (4) with ϕ held constant yields

$$\ln\left[\frac{\delta W + \Delta - \delta_{ri}}{\delta W_0 + \Delta - \delta_{ri}}\right] = \frac{-w}{W(\phi + 1)} = \frac{-\phi \bar{r} t}{W(\phi + 1)} \qquad (5)$$

where δW_0 equals the initial $\delta^{18}O$ value of seawater either before any seafloor spreading begins or directly after any instantaneous excursion in the $\delta^{18}O$ of the oceans from its steady state (buffered) value. In (5), note that the time t (in years) is implicit in w, since $w = \phi r = \phi Rct$, where R is the spreading rate in km²/yr and c is a conversion constant derived from setting a particular value for the depth of exchange (conservatively taken to be 6 km); this equation converts km³ of

rock into grams of oxygen. Exponentiating (5) and substituting ϕRct for w, we obtain

$$\delta W = (\delta W_0 + \Delta - \delta_{ri}) \exp\left[-\left(\frac{\phi}{\phi+1}\right)\frac{Rct}{W}\right] + (\delta_{ri} - \Delta) \quad (6)$$

where $\delta_{ri} - \Delta$ is identical to the steady state buffered $\delta^{18}O$ value of seawater. If Δ is exactly +5.7, then the buffered value of seawater is its present-day value, $\delta\ ^{18}O_{SW} \equiv 0$, and (6) becomes

$$\delta W = \delta W_0 \exp\left[-\left(\frac{\phi}{\phi+1}\right)\frac{Rct}{W}\right] \quad (6')$$

A result similar to that given above can be derived in a different manner by again considering the closed system water/rock equation for very large water/rock ratios (large ϕ values):

$$\frac{W}{cR} = \frac{\delta_{rf} - 5.7}{\delta W_0 - \delta W_f} \quad (7)$$

Inasmuch as the mass of the oceans greatly exceeds the mass of rock created in a single year, if we set $\Delta = 5.7$, we have $\delta_{rf} = 5.7 + \delta W_f \sim 5.7 + \delta W_0$. Then the closed system water/rock equation becomes

$$\delta W_1 = \delta W_0 (1 - cR/W) \quad (8)$$

which describes the change in the initial $\delta W_0 \neq 0$ seawater after 1 year of aging.

After 2 years,

$$\delta W_2 = \delta W_1(1 - cR/W) = \delta W_0(1 - cR/W)^2 \quad (9a)$$

For N years the equation becomes

$$\delta W_N = \delta W_0(1 - cR/W)^N \quad (9b)$$

Remembering that R is the spreading rate in years, we can perform the calculation as many times (n) per year as we wish:

$$\delta W_f = \delta W_0(1 - cR/nW)^{nt} \quad (10)$$

with t in years. As $n \to \infty$, this becomes

$$\delta W = \delta W_0 \exp\left[-\frac{cRt}{W}\right] \quad (11)$$

which is exactly the same as (6') for large ϕ. This represents the fastest rate at which seawater can be brought down to a steady state value of zero.

In Figure 10 we plot (6) for various spreading rates assuming $\Delta = 5.7$, which is the same as assuming a $\delta^{18}O_{SW} = 0$ for the steady state value. The hatched area represents the average spreading rate for the last 20 m.y. [*Berger and Winterer,* 1974] for two different values of the water/rock ratio ($\phi = 1$ or 20). The $\phi = 20$ curve represents a plausible maximum water/rock ratio for the mid-ocean ridge systems, as deduced from heat flow arguments and conservation of energy [*Wolery and Sleep,* 1976]. The $\phi = 1$ curve is probably close to the slowest plausible decay rate, assuming a simple, one-pulse injection of basaltic magma analogous to the Skaergaard hydrothermal system, where the overall water/rock ratio was about 0.5 to 1.5 [*Norton and Taylor,* 1979]. The other trajectories on Figure 10 represent transient decay for various assumed spreading rates, remembering that for today's oceans, km^2 spreading rates are roughly equivalent to half-spreading rates in cm/yr. A rate of 12 km^2/yr is used as the most plausible upper limit on the spreading rate; rates this fast have been proposed on some ridge segments during the middle Cretaceous for the period 85–115 m.y. B.P. [*Larson and Pitman,* 1972]. Such a rate is based upon extrapolating rates determined on small segments of preserved seafloor to the entire ridge system, as well as assuming that the overall ridge length is equivalent to the present-day value; thus 12 km^2/yr may be too high for any reasonable Phanerozoic worldwide rate [*Baldwin et al.,* 1974; *Berger and Winterer,* 1974].

In order to understand how increasing the spreading rate affects the buffering system, we use a plot of spreading rate versus $t_{1/2}$, the time it takes for seawater to more halfway from its initial $\delta^{18}O$ value toward its final steady state $\delta^{18}O$ value. In the inset of Figure 10 the $\phi = 1$ and $\phi = 20$ values bracket the geologically reasonable water/rock ratios for the overall system. If the spreading ratio drops below about 1 to 1.5 km^2/yr, then the buffering process would break down, and hydrothermal circulation no longer would buffer seawater. Increasing the spreading rate beyond 4–5 km^2/yr (or keeping the linear half spreading rate constant while increasing the number of plates) does not appreciably affect the $t_{1/2}$ value.

The Steady State (Buffered) $\delta^{18}O$ Value of the Oceans

Using the model described above, we can now make some estimates of the true steady state $\delta^{18}O$ value of the oceans and also estimate the average value of Δ for the seawater-crust system. The biggest obstacle in exactly determining these values is the transient effect that late Cenozoic glaciation has had upon the $\delta^{18}O$ contents of seawater. The Pleistocene paleotemperature curves of *Emiliani* [1966] are interpreted as a combination of temperature effects and isotopic shifts in seawater due to ice storage on the continents [*Dansgaard and Tauber,* 1969]. From Emiliani's data the present-day interglacial seawater isotopic composition reflects a minimum value of ice storage for the Pleistocene. During this glacial minimum, Antarctica remained covered by ice. The magnitude of the ^{18}O shift due to ice storage in Antarctica and the duration of the glaciation become the deciding factors in determining the value of Δ at times when the earth lacked any continental ice sheets. Estimates of the ^{18}O change in the oceans due to instantaneous Antarctic ice sheet formation are about +0.53 ± 0.26, based on volume estimates of 15 to 30 × 10^6 km^3 of ice having an average $\delta^{18}O$ of −33 ± 4 [*Denton et al.,* 1971; *Dansgaard and Tauber,* 1969]. This large range of estimates of ice volume and $\delta^{18}O$ compositions comes about because, during the Cenozoic, geologic evidence [*Hollister et al.,* 1976; *Hayes et al.,* 1975; *Denton et al.,* 1971; *Barker et al.,* 1976] for glaciation in Antarctica only suggests when ice sheets were present but does not record volumes. Deep Sea Drilling Project data [*Hollister et al.,* 1976] and other studies [*Denton et al.,* 1971] suggest that although minor glaciation occurred as early as the Eocene, the Antarctic continental ice sheet did not develop until the late Oligocene to middle Miocene and did not reach its present extent until late Miocene. These time constraints, together with the water/rock (ϕ) limits, fix the exponential factor in (6) at 0.76 ± 0.11 for worldwide spreading at 3 km^2/yr for the last 20 m.y. [*Berger and Winterer,* 1974]. Plugging this value into (6), we have

$$\delta^{18}O^{\text{today}}_{\text{seawater}} = \delta^{18}O_{\text{SMOW}} = 0 = (0.53 \pm 0.26) \cdot (0.76 \pm 0.11) + (5.7 \pm 0.2) - \Delta$$

Hence $\Delta = 6.1 \pm 0.3$, and at steady state the $\delta^{18}O_{\text{seawater}} = -0.40 \pm 0.3$.

The above values represent our best estimates of these im-

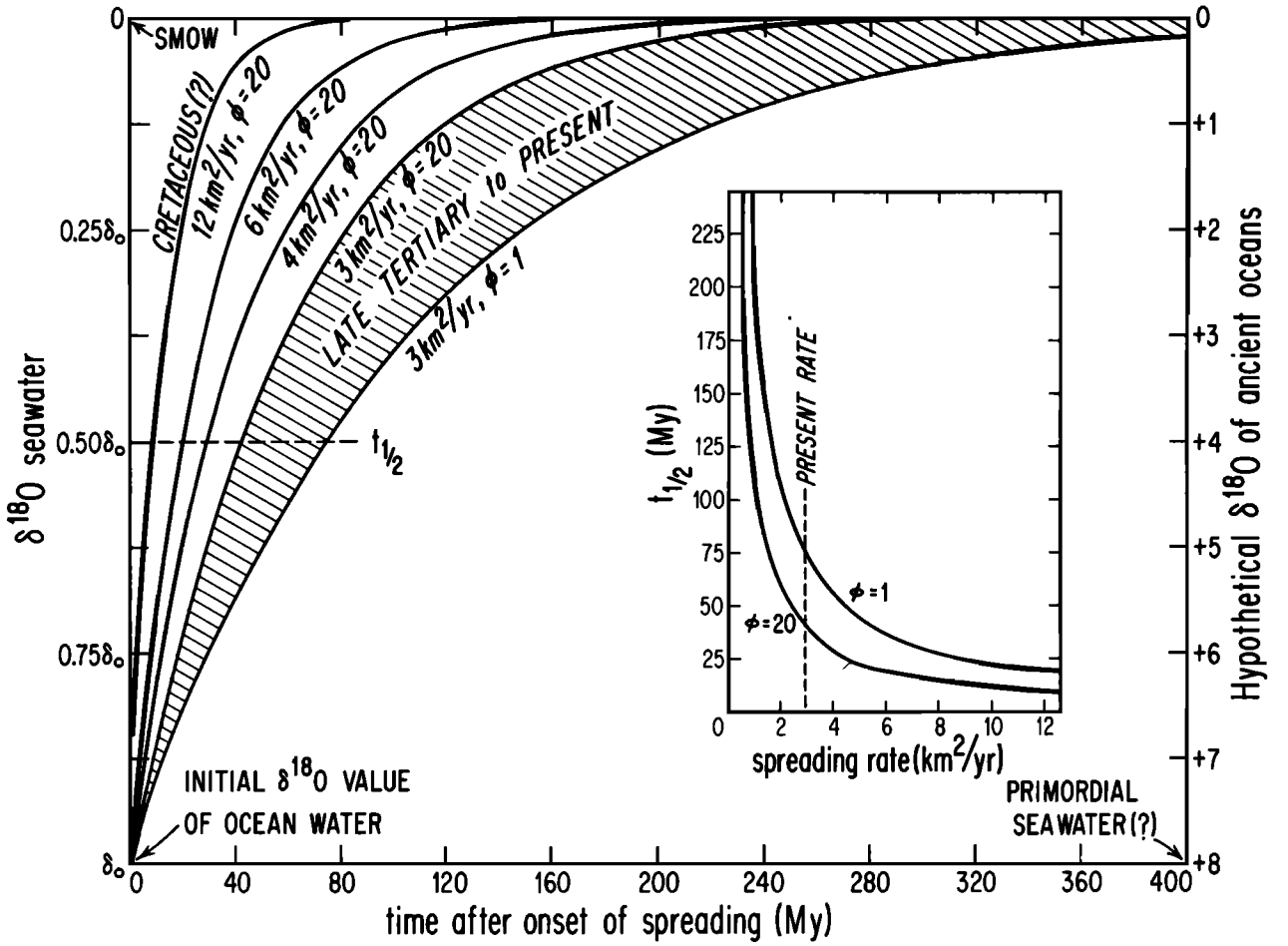

Fig. 10. Seawater isotopic evolution diagram, showing the effect of the length of time after spreading begins (t in years) on the $\delta^{18}O$ of seawater. These curves also apply equally well to rapid perturbations or excursions in the $\delta^{18}O$ of seawater, holding worldwide spreading rates constant. ϕ is the w/r ratio (in oxygen units) for the bulk system, deduced from heat flow arguments, and 12 km^2/yr is chosen as a plausible upper limit for spreading rates. Although the latter rate has been proposed for some portions of Cretaceous ocean floor, extrapolation of such high rates to a worldwide rate is very controversial [*Baldwin et al.*, 1974]. However, a rate approaching this magnitude conceivably could apply to the Archean.

portant parameters based on available information. Note, however, that the value of Δ conceivably could have been different from 6.1 if at certain time periods plate tectonic regimes were markedly different from the Phanerozoic (i.e., the Archean?). Considering another case, if the Antarctic ice sheets have existed since late Eocene, then $\Delta \sim 6.0$ and $\delta^{18}O_{\text{seawater}}^{\text{steady state}} = -0.3$. Neither this value nor the above value of -0.4 is markedly different from the value of -0.53 ± 0.26 that would be obtained by simply adding back to the oceans all of the present-day ice on earth. The point of the calculation is that the present-day $\delta^{18}O$ value of zero for mean ocean water is clearly not the steady state value. Also, simply melting all of the ice sheets and taking into account the $^{18}O/^{16}O$ effect of transferring that water back into the oceans will not necessarily give the true steady state $\delta^{18}O$ value (depending upon the duration of the glaciation). Note that it makes no difference to the buffered $\delta^{18}O$ value of ocean water whether or not the ice sheets are totally absent or even more abundant by a factor of 100 than they are today; the only consideration is whether they are waxing or waning on a scale of less than a few tens of millions of years. Because of the uncertainties in duration and particularly the magnitude of the Antarctic continental glaciation, the type of analysis outlined above probably cannot deduce the true steady state $\delta^{18}O$ value of ocean water to better than ± 0.3. This is unfortunate, since the uncertainty in seawater composition also limits the ultimate resolution of paleotemperature techniques to $\approx 3°C$ for the Mesozoic (ignoring other problems such as preservation of the isotopic record during diagenesis).

The Significance of Δ and the $\delta^{18}O$ of Precambrian Oceans

The quantity Δ represents the average ^{18}O fractionation between oceanic crust and seawater. It therefore basically reflects a weighted-average temperature of alteration of the entire section of oceanic crust and thus is related to the difference between the ambient temperature of seawater and the liquidus temperatures of the MOR magmas. The final $\delta^{18}O$ profile in the crust, which fixes the value of Δ, probably depends to a lesser extent on a number of other factors, including the geometry of the MOR magma chambers, kinetic effects, and the rates of convective circulation. However, as long as T_{magmas} and T_{seawater} are fixed and new crust is created by simple seafloor spreading (i.e., a ridge-axis magma cham-

ber capped by a roof of sheeted diabase and pillow lavas), then Δ should also remain essentially fixed.

The existence of ophiolites with similar structure and stratigraphy throughout the Phanerozoic [*Coleman,* 1977] supports the idea that oceanic crust was created by practically identical processes throughout the last 0.6 eons. Preliminary evidence from the Canyon Mountain ophiolite (Permian), $4.7 < \delta^{18}O_{\text{whole-rock}} < 11.0$, and the Bay of Islands ophiolite (Cambro-Ordovician), $4.5 < \delta^{18}O_{\text{whole-rock}} < 10.9$ [*Gregory,* 1980], compared to the more extensive data set reported here from Oman ($3.8 < \delta^{18}O_{\text{whole-rock}} < 12.7$), clearly indicates that the Paleozoic Δ value must have been very similar to the Cretaceous value and thus that seawater has been within ±1 of its steady state value at least as far back as the Cambrian. Ophiolites and/or ophiolite-like rocks of late Proterozoic age have been reported from China [*Xuchang,* 1979] and the Red Sea region [*Engel et al.,* 1978], suggesting that this statement is also probably valid as far back as 1.0–1.5 eons. However, in the ancient Precambrian record there are no reported ophiolites or preserved slices of modern types of oceanic crust.

Perry et al. [1978] have proposed that MOR hydrothermal circulation was not as important in the Precambrian as it is today. These conclusions are not reasonable in light of the evidence for deep circulation in the present study. During the early Precambrian, there was a great deal more heat production from radioactive decay, as well as more volcanism, indicating that overall heat loss to the world ocean was greater than at present, either as a result of faster spreading or because there was a much larger number of plates [*McKenzie and Weiss,* 1975]. Given our knowledge of the permeabilities of recently erupted volcanic piles [*Norton and Taylor,* 1979], it is certain that convective circulation of surface waters would have occurred on a large scale. However, because of possible differences in style of spreading, it is less certain exactly what the values of Δ and $\delta^{18}O_{SW}$ were during the early Precambrian.

Isotopic data from Precambrian cherts [*Perry et al.,* 1978; *Knauth and Epstein,* 1976; *Yeh and Epstein,* 1978] establish an upper limit for Archean ocean temperatures at less than 75°–90°C. Atmosphere models for the Precambrian [*Sagan and Mullen,* 1972] independently suggest that surface temperatures would not have been drastically higher than present-day temperatures. Volcanic rocks preserved in the Archean greenstone belts range from komatiites to rhyolites, with tholeiitic basalt as the predominant rock type [*Naldrett and Goodwin,* 1977]. This implies that the temperature difference between ocean water and submarine magmas during formation of the Archean oceanic crust should have been within ±50° to 100°C of the present-day value (which is about 1100°C). If true, this would require that both the average temperature and the average temperature range (but not the gradient!) within the hydrothermally altered oceanic crust be almost identical to the present-day value. Irrespective of the thickness of that crust the proportions of low-*T* and high-*T* alteration assemblages thus ought to be constant, as long as seawater circulates downward to within close proximity of the submarine magma chambers. However, because of overall higher temperatures that might have prevailed during hydrosphere-crust interaction in the Archean, there probably would have been less ^{18}O enrichment in the upper portion of the oceanic crust than at present (and thus there would also have to have been a concomitant smaller volume of ^{18}O-depleted rocks in the deeper parts of the oceanic crust). These effects taken together would produce a smaller Δ value. Nevertheless, Δ would have to be either very close to the present-day value or only slightly lower ($\Delta \approx 5$?), implying that ocean water probably had a constant $\delta^{18}O$ value of about −1.0 to +1.0 during almost all of earth's history.

In support of the above conclusion, ^{18}O evidence and alteration mineral assemblages from the Archean Abitibi greenstone belt [*Beaty and Taylor,* 1979] suggest that the seawater that interacted with the Archean pillow lavas had $\delta^{18}O = 0 \pm 2$. Studies of granitic rocks that were isotopically exchanged with Precambrian meteoric-hydrothermal fluids at 1.4 to 1.5 eons (St. Francois Mountains [*Wenner and Taylor,* 1976]) and at 2.6 to 3.3 eons (Swaziland and Barberton areas, South Africa [*Taylor and Magaritz,* 1975]) suggest that Precambrian meteoric waters (and thus by inference the Precambrian oceans as well) also had $\delta^{18}O$ values similar to those of the present day.

The above interpretation, suggesting relative constancy of the $\delta^{18}O$ of seawater, is in conflict with the conclusions of *Chase and Perry* [1972] and *Perry et al.* [1978, Case 1, Figure 4]. These workers proposed that the ^{18}O content of the oceans has steadily increased since ≈2.5 eons. However, their hypothesis is not valid because they dismissed the effects of deep high-*T*, hydrothermal convective circulation at spreading centers.

SUMMARY AND CONCLUSIONS

We have shown above that deep hydrothermal circulation of seawater has affected most of the feldspar-bearing rocks of the Samail ophiolite, including a large part of the section that is equivalent to oceanic layer 3. The deeper portions are depleted in ^{18}O relative to primary MOR basalts ($\delta^{18}O = +5.7$), whereas the shallower parts are enriched in ^{18}O. However, the final $\delta^{18}O$ profile in the ophiolite is the cumulative result of a long history of hydrothermal alteration, beginning with high-temperature interactions with newly formed crust at the ridge axis and continuing for at least several hundred thousand years during spreading away from the ridge axis. The earlier stages tend to produce ^{18}O depletions, whereas the later stages produce ^{18}O enrichments. We have termed the latter process 'isotopic aging,' and the ^{18}O enrichments are probably a result of two separate effects: (1) strongly ^{18}O-shifted waters that have circulated deep under the flanks of the magma chambers and then have risen upward just beyond the distal ends of the chamber (Figure 8) and (2) less ^{18}O-shifted waters with much lower temperatures that have circulated downward into the same marginal zone.

We have had some success in defining the isotopic effects produced at various stages of the isotopic aging process by looking at veining and dike relationships and by examining stoped xenoliths in the gabbros in the Samail complex. However, it must be emphasized that the final $\delta^{18}O$ profile in the ophiolite represents the superposition of a very long, complex, and continuously changing series of events in which the water/rock ratios, temperatures, $\delta^{18}O$ values of the fluids, rock permeabilities, rates of isotopic exchange, and chemical compositions of the fluids are all varying both with respect to time and with respect to position relative to the ridge axis. Without carrying out a complete numerical analysis of this problem in the manner that was done for the Skaergaard intrusion by *Norton and Taylor* [1979], we can only describe the observed isotopic effects in semiquantitative terms.

In spite of the above complexities it is worthwhile to discuss some implications of the $\delta^{18}O$ data regarding the overall time-temperature history of hydrothermal circulation in the oceanic crust. The proposed style of H_2O circulation is illustrated in cartoon fashion in Figure 8. On the basis of field mapping [*Hopson et al.*, 1981; *Hopson and Pallister*, 1979], the Samail gabbro magma chamber appears to have had a shape similar to that indicated in Figure 8. This is the basic shape proposed for the Troodos [*Greenbaum*, 1972] and Pt. Sal ophiolites [*Hopson and Frano*, 1977], and it is similar to the shape of many continental layered gabbro complexes formed in rift environments (e.g., the Muskox [*Irvine and Baragar*, 1972] and Great Dyke [*Worst*, 1960]). The floor of the magma chamber thus somewhat resembles the bottom of a wide, very long ship, with the poorly defined feeder dike system representing the keel; in this analogy the roof of the chamber is the deck of the ship. This shape probably closely approximates the geometry of the magma chamber at a fast spreading ridge. At a slow spreading ridge the 'wings' would be much smaller or nonexistent.

The result of this particular geometry is that two decoupled regimes of hydrothermal circulation must exist during most of the history of alteration. The first occurs directly over the magma chamber and is continuous across the ridge axis (this is termed the 'upper system'). The upper seawater-hydrothermal circulation system lies exclusively within the pillow lavas and the sheeted diabase-dike complex, and the H_2O penetrates downward only as far as the flat roof of the magma chamber. The water cannot penetrate any more deeply than the joint and fracture system will allow, and thus (in geologically reasonable times) the water cannot cross the diabase-magma chamber contact [*Taylor and Forester*, 1979; *Norton and Taylor*, 1979]. In fact, some H_2O is undoubtedly added to the magma from the upper system, but this must come about through dehydration of stoped blocks of hydrothermally altered roof rocks that should be abundant in such a tectonically active, rifting environment [*Taylor*, 1977; *Taylor and Forester*, 1979; *Gregory and Taylor*, 1979; *Taylor*, 1980]. Because the stratigraphic thickness of rocks above the roof of the magma chamber is very small compared to the width of the chamber, the upper hydrothermal system probably involves a large number of separate convection cells, perhaps dominated by the ridge-axis system [*Corliss et al.*, 1979]. The upper system therefore must involve very large overall water/rock ratios (>10, see *McCulloch et al.* [1981]), and the circulating seawater will be only slightly ^{18}O shifted away from its initial value.

The isotopic and alteration effects produced by the upper regime are in part destroyed or masked by later alteration effects that come about when fluids from the 'lower system' finally are able to penetrate upward into the sheeted diabase complex at the distal edges of the magma chamber. This will happen as soon as the rocks (high-level gabbros and plagiogranites) are consolidated enough to fracture. In the cartoon (Figure 8) this is indicated to occur discontinuously as small pockets of late-stage magma become isolated from one another due to the vagaries of the crystallization process in such a spreading environment. The seawater circulation system within the layered gabbro cumulates underneath the wings of the magma chamber involves very high temperatures (>400°C) and low water/rock ratios (closed system) of the order of 0.3–1.0 (weight units).

The fluid involved in the lower system is seawater that has moved laterally inward from well beyond the distal ends of the magma chamber. Because this water cannot move upward in any significant quantities directly through the liquid magma, it must either cycle (hence the closed system characteristic) or escape upward at the distal edge of the chamber when conduits in fractured, solidified rock become available at the gabbro-diabase contact (Figure 8). Both processes undoubtedly occur. Therefore large quantities of this heated and strongly ^{18}O-shifted water ($\delta^{18}O_{H_2O} = +4$ to $+8$) will be focused upward along the sloping base of the magma chamber. This H_2O will impose a final alteration event upon the sheeted dike complex, the magnitude of which will depend on the amount of focusing of hydrothermal fluid that occurs at the edge of the chamber. Note that if any water does diffuse directly into the magma from the country rocks, it must be from the lower system. It is plausible that tiny amounts of the very low density, high-T H_2O in fractures below the 'wings' of the magma chamber could diffuse upward into the overlying magma, in the manner proposed for the trough bands of the Skaergaard intrusion [*Taylor and Forester*, 1979]. The shape of the magma chamber shown in Figure 8 is, in fact, ideal for such a process to operate. The strongly ^{18}O-shifted water of the lower system also locally penetrates down into the peridotite along conjugate fractures which postdate the tectonite fabric. These waters, whose ^{18}O composition is buffered by a large reservoir of olivine with $\delta^{18}O \approx 5.7$, produce the ^{18}O enrichments of pyroxene-plagioclase pairs in gabbro dikes that were intruded along these fractures (Figures 5 and 7).

Strontium isotope data (which are not subject to temperature effects) record open system water-rock ratios (weight units) of approximately 10–30 in the sheeted dike complex [*McCulloch et al.*, 1981]. This represents the integrated effects of hydrothermal fluids of the upper system as well as of fluids derived from the lower and 'marginal' systems. Depending upon the magnitude of the $^{87}Sr/^{86}Sr$ shift in the lower system fluid, the diabase at the distal edge of the chamber may already be in approximate strontium isotope equilibrium with the fluid discharging upward from the layered gabbros (i.e., $^{87}Sr/^{86}Sr$ in diabase ≈ 0.705 [*McCulloch et al.*, 1981]). This suggests that the strontium isotopes may not be recording the final hydrothermal exchange events in the ophiolite, just as the oxygen isotopes do not record (except indirectly) the earlier exchange events in the upper system at the ridge axis. This possibly could be sorted out with more $^{87}Sr/^{86}Sr$ data on certain late-stage features such as veins and plagiogranite dikes. Because of these complex effects, the correlations between $^{87}Sr/^{86}Sr$ and $^{18}O/^{16}O$ suggested by data from *Spooner* [1977] and *McCulloch et al.* [1981] are, in some respects, fortuitous.

The style of hydrothermal circulation and the geometry of the magma chamber shown in Figure 8 imply that there should be a dramatic shift or abrupt discontinuity in the isotopic record at the gabbro-diabase contact (i.e., at the fossil roof of the magma chamber). This is in fact just what is observed, as both the $\delta^{18}O$ (Figure 3) and the $^{87}Sr/^{86}Sr$ values [*McCulloch et al.*, 1981] change very rapidly at this boundary, which must represent a discontinuity in both the average temperature of hydrothermal alteration and in the average, integrated water/rock ratio (see Table 1 and Figure 3). Part of the explanation for higher water/rock ratios in the sheeted complex is the long history of hydrothermal exchange that these rocks undergo prior to crystallization of the high-level gabbro (Figure 8). However, in addition, there is almost certainly an abrupt permeability change across the diabase-gab-

bro contact as well. The highly jointed dike complex ought to be much more permeable than the gabbros (perhaps by a factor of 10, see *Norton and Taylor* [1979]). The combination of finer grain size and higher permeability thus also contributes to the much higher effective water/rock ratios in the sheeted complex relative to the gabbros. The variations in these parameters also help to explain the preservation of the high-temperature alteration assemblages and lack of low-temperature ^{18}O exchange in the gabbros. The finer-grained, more permeable diabase dikes and pillow lavas will undergo ^{18}O exchange down to much lower temperatures than the coarser-grained, less permeable gabbros. The latter rocks exhibit such effects only along fractures and veins. We do not yet know how far beyond the distal edge of the magma chamber the ^{18}O exchange effects in the oceanic crustal section proceed at a significant rate.

Acknowledgments. We are extremely grateful to Robert G. Coleman of the U.S. Geological Survey, who first suggested this study and whose scientific guidance and expertise have been invaluable in the planning, logistics, and field work in Oman in 1977 and 1978. This work is part of a cooperative study carried out with C. A. Hopson, E. H. Bailey, and J. S. Pallister, who have also contributed greatly to our understanding of the geology and petrology of the Oman Mountains. A few additional samples were provided by R. G. Coleman. We particularly want to thank R. E. Criss for numerous discussions, including his help in clarifying the nature of the plagioclase-pyroxene $\delta^{18}O$ exchange phenomena. We also thank M. T. McCulloch, D. Beaty, and S. Epstein for stimulating discussions of this work. Financial support for this study came from the National Science Foundation, grants EAR-76-21310 and EAR-7816874, and the Department of Energy, grant EX-76-G-03-1305, to H.P.T., as well as a National Science Foundation grant to C. A. Hopson for field work in Oman. Additional support for R.T.G. came from a graduate fellowship from the Continental Oil Company and from a Penrose Grant from the Geological Society of America for field work in 1979. Field vehicles were provided by the California Institute of Technology and by Petroleum Development (Oman) Ltd. We gratefully acknowledge the Ministry of Agriculture, Fisheries, Petroleum, and Minerals and especially the Directorate General of Petroleum and Minerals, Sultanate of Oman, for their help and sponsorship of this study. Contribution 3284, Division of Geological and Planetary Sciences, California Institute of Technology.

REFERENCES

Anderson, A. T., R. N. Clayton, and T. K. Mayeda, Oxygen isotope geothermometry of mafic igneous rocks, *J. Geol., 79,* 715–729, 1971.

Baldwin, B., P. J. Coney, and W. R. Dickinson, Dilemma of a Cretaceous time scale and rates of sea-floor spreading, *Geology, 2,* 267–270, 1974.

Barker, P. F., et al., *Initial Reports of Deep Sea Drilling Project,* vol. 36, 1080 pp., U.S. Government Printing Office, Washington, D. C., 1976.

Barnes, I., J. R. O'Neil, and J. J. Trescases, Present day serpentinization in New Caledonia, Oman and Yugoslavia, *Geochim. Cosmochim. Acta, 42,* 144–145, 1978.

Beaty, D. W., and H. P. Taylor, Jr., Oxygen isotope geochemistry of the Abitibi greenstone belt, Ontario: Evidence for seawater/rock interaction and implications regarding the isotopic composition and evolution of the ocean and oceanic crust, *Geol. Soc. Amer. Abstr. Programs, 11,* 386, 1979.

Berger, W. H., and E. L. Winterer, Plate stratigraphy and the fluctuating carbonate line, Pelagic Sediments on Land and Under the Sea, *Int. Ass. Sedimentol. Spec. Publ., 1,* 11–48, 1974.

Boudier, F., and R. G. Coleman, Cross section through the peridotite in the Samail ophiolite, Oman, southeastern Oman Mountains, *J. Geophys. Res., 86,* this issue, 1981.

Chase, C. G., and E. C. Perry, Jr., The oceans: Growth and oxygen isotope evolution, *Science, 177,* 992–994, 1972.

Coleman, R. G., *Ophiolites: Ancient Oceanic Lithosphere?,* Springer, New York, 1977.

Coleman, R. G., Tectonic setting for ophiolite obduction in Oman, *J. Geophys. Res., 86,* this issue, 1981.

Corliss, J. B., J. Dymond, L. I. Gordon, J. M. Edmond, R. P. von Herzen, R. D. Ballard, K. Green, D. Williams, A. Bainbridge, K. Crane, and T. H. Van Andel, Submarine thermal springs on the Galapagos Rift, *Science, 203,* 1073–1083, 1979.

Dansgaard, W., and H. Tauber, Glacier oxygen-18 content and Pleistocene ocean temperatures, *Science, 166,* 499–502, 1969.

Denton, G. H., R. L. Armstrong, and M. Stuiver, The late Cenozoic glacial history of Antarctica, in *The Late Cenozoic Glacial Ages,* edited by K. K. Turekian, pp. 267–304, Yale University Press, New Haven, 1971.

Edmond, J. M., H. Craig, L. I. Gordon, and H. D. Holland, Chemistry of hydrothermal waters at 21°N on the East Pacific Rise, *Eos Trans. AGU, 60,* 864, 1979.

Emiliani, C., Isotopic paleotemperatures, *Science, 154,* 851–857, 1966.

Engel, A. E. J., T. H. Dixon, R. J. Stern, E. M. El Shazly, and A. Abdullah, Geologic evolution of northeast Africa, *Geol. Soc. Amer. Abstr. Programs, 10,* 396, 1978.

Forester, R. W., and H. P. Taylor, Jr., $^{18}O/^{16}O$, D/H, and $^{13}C/^{12}C$ studies of the Tertiary igneous complex of Skye, Scotland, *Amer. J. Sci., 277,* 136–177, 1977.

Glennie, K. W., M. G. A. Bouef, M. W. Hughes Clark, M. Moody-Stuart, W. F. H. Pilaar, and B. M. Reinhardt, Geology of the Oman Mountains, *Trans. Roy. Dutch Geol. Mining Soc., 31,* 423, 1974.

Godfrey, J. D., The deuterium content of hydrous minerals from the east-central Sierra Nevada, and Yosemite National Park, *Geochim. Cosmochim. Acta, 26,* 1215–1245, 1962.

Greenbaum, D., Magmatic processes at ocean ridges: Evidence from the Troodos Massif, Cyprus, *Nature, 238,* 18–21, 1972.

Gregory, R. T., Oxygen and hydrogen isotope study of the Samail ophiolite, Oman: Implications for origin and hydrothermal alteration of the oceanic crust, Ph.D. thesis, Calif. Inst. of Technol., Pasadena, Calif., 1980.

Gregory, R. T., and H. P. Taylor, Jr., Oxygen isotope and field studies applied to the origin of oceanic plagiogranites, paper presented at the International Ophiolite Symposium, Geol. Surv. Dep. of Cyprus, Nicosia, 1979.

Hayes, D. E., et al., *Initial Reports of Deep Sea Drilling Project,* vol. 28, U.S. Government Printing Office, Washington, D. C., 1975.

Heaton, T. H. E., and S. M. F. Sheppard, Hydrogen and oxygen isotope evidence for seawater hydrothermal alteration and ore deposition, Troodos complex. Cyprus, Volcanic Processes in Ore Genesis, *Spec. Pap. 7,* pp. 42–57, Geol. Soc. of London, London, 1977.

Hollister, C. D., *Initial Reports of Deep Sea Drilling Project,* vol. 35, 930 pp., U.S. Government Printing Office, Washington, D. C., 1976.

Hopson, C. A., and C. J. Frano, Igneous history of the Point Sal ophiolite, southern California, North American Ophiolites, *Oreg. Dep. Geol. Miner. Resour. Bull., 95,* 161–183, 1977.

Hopson, C. A., and J. S. Pallister, Samail ophiolite magma chamber, I, Evidence from gabbro phase variation, internal structure and layering, paper presented at the International Ophiolite Symposium, Geol. Surv. Dep. of Cyprus, Nicosia, 1979.

Hopson, C. A., R. G. Coleman, R. T. Gregory, J. S. Pallister, and E. H. Bailey, Geologic section through the Samail ophiolite and associated rocks along a Muscat-Ibra transect, southeastern Oman Mountains, *J. Geophys. Res., 86,* this issue, 1981.

Irvine, T. N., and W. R. A. Baragar, Muskox intrusion and Coppermine River lavas Northwest Territories, *Int. Geol. Congr. 24, 70,* 1972.

Knauth, L. P., and S. Epstein, Hydrogen and oxygen isotope ratios in nodular and bedded cherts, *Geochim. Cosmochim. Acta, 40,* 1095–1108, 1976.

Lanphere, M. A., K-Ar ages of metamorphic rocks at the base of the Samail ophiolite, Oman, *J. Geophys. Res., 86,* this issue, 1981.

Larson, R. L., and W. L. Pitman III, Worldwide correlation of Mesozoic magnetic anomalies, and its implications, *Geol. Soc. Amer. Bull., 83,* 3645–3662, 1972.

Magaritz, M., and H. P. Taylor, Jr., Oxygen and hydrogen isotope studies of serpentinization in the Troodos ophiolite complex, Cyprus, *Earth Planet. Sci. Lett., 23,* 8–14, 1974.

Magaritz, M., and H. P. Taylor, Jr., Oxygen, hydrogen and carbon isotope studies of the Franciscan formation, Coast Ranges, California, *Geochim. Cosmochim. Acta, 40,* 215–234, 1976*a*.

Magaritz, M., and H. P. Taylor, Jr., $^{18}O/^{16}O$ and D/H studies along a

500 km traverse across the Coast Range batholith and its country rocks, central British Columbia, *Can. J. Earth Sci., 13,* 1514–1536, 1976*b*.

McCulloch, M. T., R. T. Gregory, G. J. Wasserburg and H. P. Taylor, Jr., A neodymium, strontium, and oxygen isotopic study of the Cretaceous Samail ophiolite and implications for the petrogenesis and seawater-hydrothermal alteration of oceanic crust, *Earth Planet. Sci. Lett., 46,* 201–211, 1980.

McCulloch, M. T., R. T. Gregory, G. J. Wasserburg, and H. P. Taylor, Jr., Sm-Nd, Rb-Sr, and $^{18}O/^{16}O$ isotopic systematics in an oceanic crustal section: Evidence from the Samail ophiolite, *J. Geophys. Res., 86,* this issue, 1981.

McKenzie, D. P., and N. Weiss, Speculations on the thermal and tectonic history of the Earth, *Geophys. J. Roy. Astron. Soc., 42,* 131, 1975.

Melson, W. G., and T. H. Van Andel, Metamorphism in the Mid-Atlantic ridge 22°N latitude, *Mar. Geol., 4,* 165–186, 1966.

Muehlenbachs, K., and R. N. Clayton, Oxygen isotope ratios of submarine diorites and their constitutent minerals, *Can. J. Earth Sci., 8,* 1591–1595, 1971.

Muehlenbachs, K., and R. N. Clayton, Oxygen isotope studies of fresh and weathered submarine basalts, *Can. J. Earth Sci., 9,* 172–184, 1972*a*.

Muehlenbachs, K., and R. N. Clayton, Oxygen isotope geochemistry of submarine Greenstones, *Can. J. Earth Sci., 9,* 471–478, 1972*b*.

Muehlenbachs, K., and R. N. Clayton, Oxygen isotope composition of the oceanic crust and its bearing on seawater, *J. Geophys. Res., 81,* 4365–4369, 1976.

Muehlenbachs, K., A. T. Anderson, and G. E. Sigvaldason, Low-^{18}O basalts from Iceland, *Geochim. Cosmochim. Acta, 38,* 577–588, 1974.

Naldrett, A. J., and A. M. Goodwin, Volcanic rocks of the Blake River Group, Abitibi greenstone belt, Ontario, and their sulfur content, *Can. J. Earth Sci., 14,* 539–550, 1977.

Nicolas, A., F. Boudier, and J.-L. Bouchez, Interpretation of peridotite structures from ophiolitic and oceanic environments, *Amer. J. Sci.,* in press, 1980.

Norton, D., and H. P. Taylor, Jr., Quantitative simulation of the hydrothermal systems of crystallizing magmas on the basis of transport theory and oxygen isotope data: An analysis of the Skaergaard intrusion, *J. Petrology, 20,* 421–486, 1979.

O'Neil, J. R., and H. P. Taylor, Jr., The oxygen isotope cation exchange chemistry of feldspars, *Amer. Mineral., 52,* 1414–1437, 1967.

Onuma, N., R. N. Clayton, and T. K. Mayeda, Apollo 11 rocks: Oxygen isotope fractionation between minerals and an estimate of the temperature of formation, *Geochim. Cosmochim. Acta,* Suppl. 1, *2,* 1429–1434, 1970.

Perry, E. C., Jr., S. N. Ahmad, and T. M. Swulius, The oxygen isotope composition of 3,800 m.y. old metamorphosed chert and iron formation from Isukasia, West Greenland, *J. Geol., 86,* 223–239, 1978.

Reinhardt, B. M., On the genesis and emplacement of ophiolites in the Oman Mountains geosyncline, *Schweiz. Mineral. Petrogr. Mitt., 49,* 1–30, 1969.

Sagan, C., and G. Mullen, Earth and Mars: Evolution of atmospheric and surface temperatures, *Science, 177,* 52–56, 1972.

Spooner, E. T. C., Hydrodynamic model for the origin of the ophiolitic cupriferous pyrite ore deposits of Cyprus, *Geol. Soc. London Spec. Publ., 7,* 58–72, 1977.

Spooner, E. T. C., R. D. Beckinsale, W. S. Fyfe, and J. D. Smewing, ^{18}O-enriched ophiolitic metabasic rocks from E. Liguria, Pindos and Troodos, *Contrib. Mineral. Petrol., 47,* 41–62, 1974.

Steiner, J., and E. Grillman, Possible galactic causes for periodic and episodic glaciations, *Geol. Soc. Amer. Bull., 84,* 1003–1018, 1973.

Stern, C., M. J. de Wit, and J. R. Lawrence, Igneous and metamorphic processes associated with the formation of Chilean ophiolites and their implication for ocean floor metamorphism, seismic layering and magnetism, *J. Geophys. Res., 81,* 4370–4380, 1976.

Taylor, H. P., Jr., The oxygen isotope geochemistry of igneous rocks, *Contrib. Mineral. Petrol., 19,* 1–71, 1968.

Taylor, H. P., Jr., Oxygen isotope evidence for large-scale interaction between meteoric ground waters and Tertiary granodiorite intrusions, western Cascade Range, Oregon, *J. Geophys. Res., 76,* 7855–7874, 1971.

Taylor, H. P., Jr., Water/rock interactions and the origin of H_2O in granite batholiths, *J. Geol. Soc. London, 133,* 509–558, 1977.

Taylor, H. P., Jr., Stable isotope studies of spreading centers and their bearing on the origin of granophyres and plagiogranites, in *Proceedings of the International Meeting of Mafic-Ultramafic Association in Orogenic Belts,* edited by C. Allegre, Centre National de Recherche Scientifique, Grenoble, France, in press, 1980.

Taylor, H. P., Jr., and R. G. Coleman, Oxygen isotopic evidence for meteoric-hydrothermal alteration of the Jabal at Tirf complex, Saudi Arabia (abstract), *Eos Trans. AGU, 58,* 516, 1977.

Taylor, H. P., Jr., and S. Epstein, Relationships between $^{18}O/^{16}O$ ratios in coexisting minerals of igneous and metamorphic rocks, *Geol. Soc. Amer. Bull., 73,* 461–480, 675–694, 1962.

Taylor, H. P., Jr., and S. Epstein, $^{18}O/^{16}O$ ratios of Apollo 11 lunar rocks and minerals, *Geochim. Cosmochim. Acta,* Suppl. 1, *2,* 1613–1626, 1970.

Taylor, H. P., Jr., and R. W. Forester, Low-^{18}O igneous rocks from the intrusive complexes of Skye, Mull, and Ardnamurchan, western Scotland, *J. Petrology, 12,* 465–497, 1971.

Taylor, H. P., Jr., and R. W. Forester, An oxygen and hydrogen isotope study of the Skaergaard Intrusion and its country rocks: A description of a 55 m.y. old fossil hydrothermal system, *J. Petrology, 20,* 355–419, 1979.

Taylor, H. P., Jr., and M. Magaritz, Oxygen and hydrogen isotope studies of 2.6–3.4 b.y. old granites from the Barberton Mountain Land, Swaziland, and the Rhodesian cration, Southern Africa, *Geol. Soc. Amer. Abstr. Programs, 7,* 1293, 1975.

Tilton, G. R., C. A. Hopson, and J. E. Wright, Uranium-lead isotopic ages of the Samail ophiolite, Oman, with applications to Tethyan ocean ridge tectonics, *J. Geophys. Res., 86,* this issue, 1981.

Wenner, D. B., and H. P. Taylor, Jr., Oxygen and hydrogen isotope studies of a Precambrian granite-rhyolite terrane, St. Francois Mountains, southeastern Missouri, *Geol. Soc. Amer. Bull., 87,* 1587–1598, 1976.

Wenner, D. B., and H. P. Taylor, Jr., Oxygen and hydrogen isotope studies of the serpentinization of ultramafic rocks in oceanic environments and continental ophiolite complexes, *Amer. J. Sci., 273,* 207–239, 1978.

Williams, H., and J. Malpas, Sheeted dikes and brecciated dike rocks within transported igneous complex, Bay of Islands, western Newfoundland, *Can. J. Earth Sci., 9,* 1216–1229, 1976.

Wolery, T. J., and N. H. Sleep, Hydrothermal circulation and geochemical flux at mid-ocean ridges, *J. Geol., 84,* 249–275, 1976.

Worst, B. G., The great dyke of Southern Rhodesia, *S. Rhodesia Geol. Surv. Bull., 47,* 234, 1960.

Xuchang, X., Ophiolite suites of China and their tectonic significance, paper presented at the International Ophiolite Symposium, Geol. Surv. Dep. of Cyprus, Nicosia, 1979.

Yeh, H.-W., and S. Epstein, D/H and $^{18}O/^{16}O$ ratios of Precambrian cherts of Swaziland sequence and others (abstract), *Eos Trans. AGU, 59,* 386, 1978.

(Received August 12, 1979;
accepted November 26, 1979.)